ISSN 1916-6117 (online)
ISBN 978-1-4868-5604-6 (PDF)

ISSN 0826-9580 (print)
ISBN 978-1-4868-5603-9 (print)

Ontario

Ontario Geological Survey
Open File Report 6377

Volcanic Stratigraphy of the Western Schreiber–Hemlo Greenstone Belt and the Mesoproterozoic Geology of the North Shore of Lake Superior, Terrace Bay Area, Northwestern Ontario

2022

Ontario

ONTARIO GEOLOGICAL SURVEY

Open File Report 6377

Volcanic Stratigraphy of the Western Schreiber–Hemlo Greenstone Belt and the Mesoproterozoic Geology of the North Shore of Lake Superior, Terrace Bay Area, Northwestern Ontario

by

S.J. Magnus

2022

Magnus, S.J. 2022. Volcanic stratigraphy of the western Schreiber–Hemlo greenstone belt and the Mesoproterozoic geology of the north shore of Lake Superior, Terrace Bay area, northwestern Ontario; Ontario Geological Survey, Open File Report 6377, 40p.

Users of OGS products should be aware that Indigenous communities may have Aboriginal or treaty rights or other interests that overlap with areas of mineral potential and exploration.

ISBN 978-1-4868-5603-9 (print)
ISBN 978-1-4868-5604-6 (PDF)

Open File Reports of the Ontario Geological Survey are available for viewing at the John B. Gammon Geoscience Library in Sudbury and at the regional Mines and Minerals office whose district includes the area covered by the report (see below).

Copies can be purchased at Publication Sales and the office whose district includes the area covered by the report. Although a particular report may not be in stock at locations other than the Publication Sales office in Sudbury, they can generally be obtained within 3 working days. All telephone, fax, mail and e-mail orders should be directed to the Publication Sales office in Sudbury. Purchases may be made using cash, debit card, VISA, MasterCard, cheque or money order. Cheques or money orders should be made payable to the *Minister of Finance*.

John B. Gammon Geoscience Library 933 Ramsey Lake Road, Level A3 Sudbury, Ontario P3E 6B5	Tel:	(705) 670-5614
Publication Sales 933 Ramsey Lake Rd., Level A3 Sudbury, Ontario P3E 6B5	Tel: Toll-free: Fax: E-mail:	(705) 670-5691 (local) 1-888-415-9845 ext. 5691 (705) 670-5770 pubsales.ndm@ontario.ca

Regional Mines and Minerals Offices:

Kenora – Suite 104, 810 Robertson St., Kenora P9N 4J2

Kirkland Lake – 1451 Hwy. 66, P.O. Box 40, Swastika P0K 1T0

Red Lake – 227 Howey Street, P.O. Box 324, Red Lake P0V 2M0

Sault Ste. Marie – 740 Great Northern Rd., Sault Ste. Marie P6B 0B4

Southern Ontario – P.O. Bag Service 43, 126 Old Troy Rd., Tweed K0K 3J0

Sudbury – 933 Ramsey Lake Rd., Level A3, Sudbury P3E 6B5

Thunder Bay – Suite B002, 435 James St. S., Thunder Bay P7E 6S7

Timmins – Ontario Government Complex, P.O. Bag 3060, 5520 Hwy. 101 East, South Porcupine P0N 1H0

Cette publication est disponible en anglais seulement.

Parts of this report may be quoted if credit is given. It is recommended that reference be made in the following form:

Magnus, S.J. 2022. Volcanic stratigraphy of the western Schreiber–Hemlo greenstone belt and the Mesoproterozoic geology of the north shore of Lake Superior, Terrace Bay area, northwestern Ontario; Ontario Geological Survey, Open File Report 6377, 40p.

Contents

FIGURES

TABLES

Abstract

The western Schreiber–Hemlo greenstone belt was the subject of a regional 1:20 000 scale bedrock mapping project during the field seasons of 2015, 2016, 2017 and 2018 that encompassed Priske, Strey, Syine, Tuuri and Walsh townships. The objective of this project was to update our understanding of the geological history of this part of the greenstone belt and its relationship to the nearby greenstone belts of the Wawa–Abitibi terrane utilizing modern geochemical and geochronological techniques. This report summarizes the results of this investigation, including descriptions of the geochemical characteristics of the volcanic rocks in the greenstone belt, presenting a stratigraphic model for the greenstone belt, and by providing a brief interpretation of the tectonic settings in which the volcanic rocks of the greenstone belt were generated. In addition, the geochemical characteristics of 3 Mesoproterozoic dike swarms present in the study area are described, along with a brief interpretation of the tectonic settings in which these dikes were formed. The data presented herein can be used as a framework for more detailed mineral exploration and academic activities in the western Schreiber–Hemlo greenstone belt specifically, and more generally, throughout the western Wawa-Abitibi terrane.

Volcanic Stratigraphy of the Western Schreiber–Hemlo Greenstone Belt and the Mesoproterozoic Geology of the North Shore of Lake Superior, Terrace Bay Area, Northwestern Ontario

S.J. Magnus[1]

Ontario Geological Survey
Open File Report 6377
2022

---

[1]**Geoscientist, Earth Resources and Geoscience Mapping Section, Ontario Geological Survey**
Seamus.magnus@ontario.ca

Introduction

This publication provides a summary of the results of part of a multiyear study of the western Schreiber–Hemlo greenstone belt, which was the subject of a regional 1:20 000 scale bedrock mapping project during the field seasons of 2015, 2016, 2017 and 2018 (OGS projects PU15-004, NW-16-003, NW-17-002, NW-18-001 and NW-19-002). The objective of this multiyear study was to update our understanding of the geological history of this part of the greenstone belt and its relationship to nearby greenstone belts of the Wawa–Abitibi terrane utilizing modern geochemical and geochronological techniques.

By gathering new field data and applying modern analytical techniques, the goal of this multiyear study was to produce updated information for the greenstone belt to be used as a framework for more detailed mineral exploration and academic activities.

Additional publications related to this multiyear study include Preliminary Maps (P.3812, P.3826, P.3845 and P.3846; Magnus 2017a, Magnus 2019a, Magnus 2021a and Hastie and Magnus 2021a, respectively), Miscellaneous Release—Data (MRD 361, MRD 375, MRD 379, MRD 381, and MRD 382; Magnus 2018, 2019b; Arnold, Hollings and Magnus 2020; Magnus 2021b; Hastie and Magnus 2021b, respectively), *Summary of Field Work and Other Activities* articles in 2015, 2016, 2017 and 2018 (Magnus and Walker 2015; Magnus and Arnold 2016; Magnus 2017b; Arnold, Hollings and Magnus 2017; Magnus and Hastie 2018), and a geological guidebook (OFR 6357; Magnus 2019c).

The summary presented herein is divided into 2 parts. Part 1 focusses on the Archean geology of the study area and includes descriptions of the geochemical characteristics of the volcanic rocks in the greenstone belt and presents a stratigraphic model for the greenstone belt. Part 2 focusses on the Mesoproterozoic geology of the study area, specifically the geochemical characteristics of 3 Mesoproterozoic dike swarms present in the study area and a brief interpretation of the tectonic settings in which these dikes were formed. The results reported herein were briefly outlined in 2 oral presentations given at the 2021 Institute on Lake Superior Geology (ILSG) annual meeting (Magnus 2021c, 2021d).

Regional Geological Setting

The bedrock along the north shore of Lake Superior hosts rocks spanning roughly 1.9 billion years of Earth's history, from the beginning of the Mesoarchean Era to the end of the Mesoproterozoic Era, and include a diverse range of rocks formed in a variety of tectonic settings.

THE WESTERN SCHREIBER–HEMLO GREENSTONE BELT

The western Schreiber–Hemlo greenstone belt is a roughly 50 km long belt of supracrustal and intrusive rocks bounded on its north and west sides by Archean granitoid plutonic rocks. It extends southward under Lake Superior and is separated from the eastern Schreiber–Hemlo greenstone belt by the Mesoproterozoic Coldwell alkalic intrusive complex (Figure 1). The greenstone belt is apparently connected to a greenstone belt in the Winston Lake–Big Duck Lake area to the north by a north-trending sliver of greenstone, but the relationship between Schreiber–Hemlo greenstone belt and the Archean metavolcanic rocks on the Slate Islands, 10 km to the south, is unknown (*see* Figure 1).

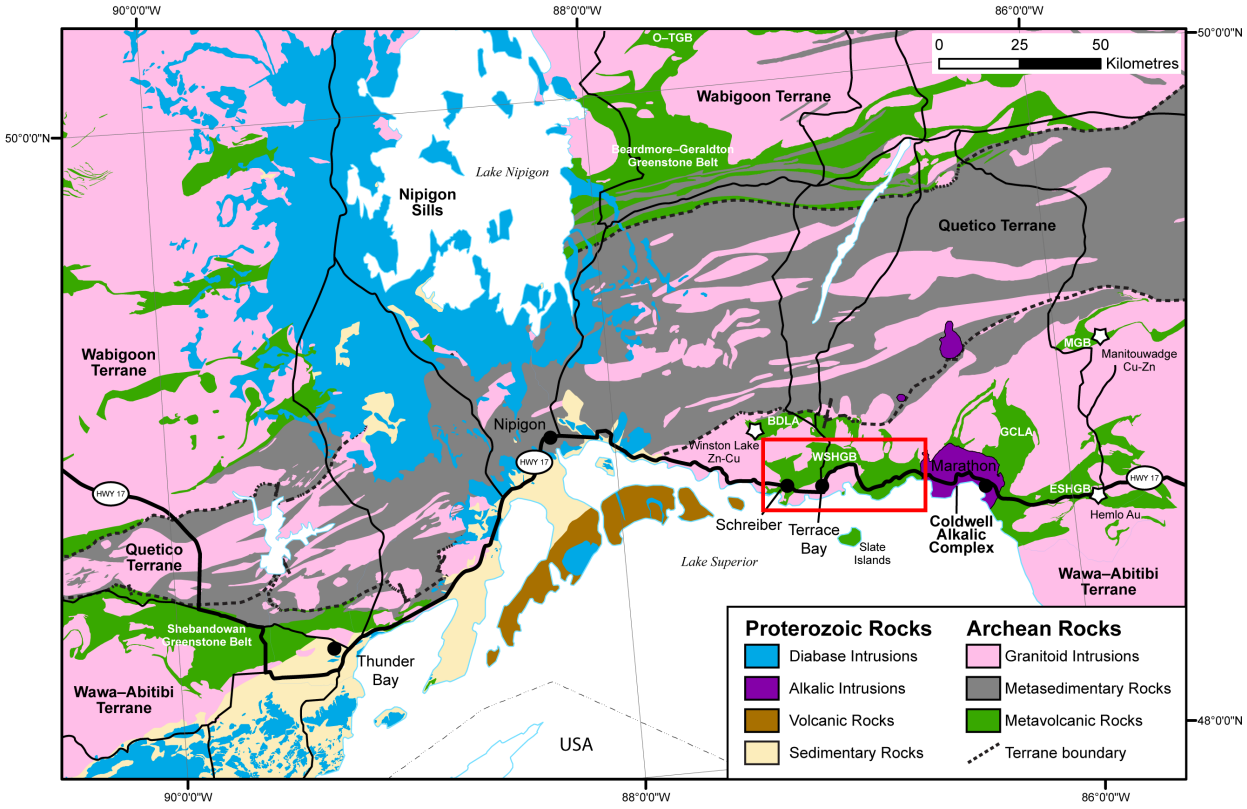

Figure 1. Regional map of the north shore of Lake Superior, displaying Archean and Proterozoic geology. White stars indicate local past-producing and currently producing mines. Abbreviations: BDLA, Big Duck Lake area; GCLA, Goodchild Lake area; O–TGB, Onaman–Tashota greenstone belt; MGB, Manitouwadge greenstone belt; ESHGB, Eastern Schreiber–Hemlo greenstone belt; WSHGB, Western Schreiber–Hemlo greenstone belt; HWY 17, Trans-Canada Highway 17. Geology *from* Ontario Geological Survey (2011); Terrane and domain boundaries *from* Stott et al. (2010). The project area related to this report is outlined in red.

NEOARCHEAN GEOLOGICAL SETTING

The Superior Province is an Archean craton that forms part of the North American continental shield. Rocks of the Superior Province, which range in age from *circa* 3400 Ma to 2600 Ma, are arranged in greenstone belts and plutonic domains. The Superior Province has been subdivided into terranes in which the rocks share similar lithological, geochemical, age and isotopic characteristics and structural and metamorphic histories (Stott et al. 2010). The relationship between these terranes during the early stages of their formation is unclear; however, the histories of their evolution converge at *circa* 2700 Ma, when the terranes were amalgamated to form the Superior craton (Stott et al. 2010).

Three major terranes are present near the north shore of Lake Superior: the Wawa–Abitibi terrane to the south, the Wabigoon terrane to the north, and the Quetico terrane between them (Figure 1). The Wawa–Abitibi granite-greenstone terrane contains Neoarchean volcanic rocks erupted through juvenile oceanic crust and is interpreted to represent an oceanic arc depositional environment (Williams 1989). The Wabigoon granite-greenstone terrane contains Neoarchean volcanic rocks erupted through and deposited upon Mesoarchean crust; it is interpreted to represent a continental arc depositional environment and is considered to have been a "protocontinent" (Williams 1989). The Quetico terrane is composed mainly of turbiditic siliciclastic rocks with sparse slivers of oceanic crust and is interpreted to

represent an accretionary wedge deposited offshore of the Wabigoon "protocontinent" (Williams 1989; Fralick, Purdon and Davis 2006).

Sedimentary rocks in the Manitouwadge greenstone belt and in the western Schreiber–Hemlo greenstone belt, both along the northern margin of the Wawa–Abitibi terrane (*see* Figure 1), contain detrital zircon populations that are correlative with those in the Quetico Terrane and in the Beardmore–Geraldton greenstone belt (Zaleski, van Breemen and Peterson 1999; Fralick, Purdon and Davis 2006; Tóth 2018, Tóth et al. 2015). This suggests that during deposition of the sedimentary sequences, the Wabigoon, Quetico and Wawa–Abitibi terranes were a contiguous depositional environment.

In this interpreted environment, detrital material from both the ongoing Wabigoon continental arc volcanism and from erosion of Mesoarchean crust of the Wabigoon "protocontinent" was deposited into a fore-arc accretionary wedge. As the Wawa–Abitibi oceanic arc approached the protocontinent, sediments from the continent began to fill the basin between them, eventually spilling over onto the still-active Wawa–Abitibi volcanic arc (Fralick, Purdon and Davis 2006).

The end of supracrustal rock formation in the northern Lake Superior region is marked at *circa* 2690 Ma by crosscutting felsic plutons (*see* Figure 1); plutonism in the region was accompanied by regional deformation and metamorphism from *circa* 2690 to *circa* 2670 Ma. The 3 terranes were deformed synchronously during 3 main events: 1) early thrusting during collision of the terranes (D_1), 2) upright folding during continued compression (D_2), and 3) late transpressional shearing (D_3) (Williams 1989). These deformational events likely represent a succession of different styles of deformation during a single protracted event, not 3 distinct events (Williams 1989).

The proposed structural histories for the Shebandowan (Corfu and Stott 1998) and Manitouwadge greenstone belts (Zaleski, van Breemen and Peterson 1999) and the eastern part of the Schreiber–Hemlo greenstone belt (Muir 2003) are similar to Williams' (1989) broad interpretation for the region; however, the timing and development of deformation is slightly different for each greenstone belt and within each terrane. These differences are likely caused by uncertainties in the geochronological data, inconsistencies in interpretations of all of the geological and related data, and the diachronous nature of regional deformation itself (Corfu and Stott 1998).

PALEOPROTEROZOIC GEOLOGICAL SETTING

Several Paleoproterozoic mafic dike swarms are present in the area north of Lake Superior, including dikes from the Matachewan (2480–2445 Ma, Heaman 1997), Biscotasing (2175–2166 Ma, Buchan, Mortensen and Card 1993; Davis and Stott 2003; Halls and Davis 2004; Hamilton and Stott 2008) and Marathon (2122–2100 Ma, Halls et al. 2008) dike swarms.

Sedimentary rocks of the Animikie Group unconformably overly the Superior Craton and the Paleoproterozoic dike swarms (*see* Figure 1). The base of the Animikie Group is defined by a thin, locally developed Kakabeka Conglomerate, which hosts carbonaceous microfossils (*Gunflintia* and *Huronosporia*) preserved in cherty stromatolites, interpreted to have formed in nearshore and shallow water environments (e.g., Wacey et al. 2013). These rocks are overlain by iron formation, carbonate rocks and siliciclastic rocks of the Gunflint Formation, which is interpreted to have been deposited during multiple marine transgressions in an extensional basin between the Penokean volcanic arc and the Superior Craton prior to their collision at *circa* 1860 Ma (Fralick, Davis and Kissin 2002) or, alternatively, in a foreland basin north of the Penokean fold-thrust belt (Ojakangas, Morey and Southwick 2001). The Gunflint Formation is overlain by fine-grained argillites and slates of the Rove Formation, which contain a mixture of Archean-age zircons and zircons *circa* 1830–1770 Ma in age (Heaman and

Easton 2006) and are interpreted to have been deposited in a deep marine setting between the assembled Laurentian Craton and the Yavapai volcanic arc (*circa* 1800–1700 Ma)(Whitmeyer and Karlstrom 2007). The boundary between the Gunflint Formation and the Rove Formation, and their lithostratigraphic equivalents in the USA, is marked by an unusual rock unit thought to represent distal ejecta from the Sudbury impact (*circa* 1850 Ma)(Addison et al. 2005; Cannon et al. 2010).

MESOPROTEROZOIC GEOLOGICAL SETTING

The Sibley Group (*circa* 1400 Ma), a sequence of sediments deposited in alluvial–fluvial, lacustrine and eolian settings, unconformably overlies the Paleoproterozoic Animikie Group (Rogala, Fralick and Metsaranta 2005).

The Keweenawan Midcontinent Rift event (*circa* 1100 Ma) caused widespread magmatic activity in the Lake Superior area. Intrusive rocks emplaced prior to rifting and which are preserved north of Lake Superior, include the Prairie Lake carbonatite-ijolite complex (*circa* 1157–1164 Ma)(Rukhlov and Bell 2010; Wu et al. 2017) and mafic to ultramafic intrusions (1120–1110 M) such as the Thunder Bay North intrusive complex, the Kitto and Seagull intrusions, and the Logan diabase sills (Bleeker et al. 2018, 2020 and references therein). Most of the preserved rift-related rocks were emplaced between 1109 and 1093 Ma and include both intrusive and supracrustal rocks, including the Osler Volcanic Group, the Nipigon and Inspiration diabase sills and the Coldwell alkalic intrusive complex (*circa* 1108 Ma)(Bleeker et al. 2018, 2020; Liikane et al. 2018, and references therein). Younger dike rocks include the Pigeon River and Cloud River dike swarms (*circa* 1099–1095 Ma; Liikane et al. 2018). The supracrustal rocks include several packages of mafic and felsic volcanic rocks and sedimentary rocks, which are overlain by late-rift volcanic and sedimentary rocks as young as *circa* 1083 Ma (Miller and Nicholson 2013 and references therein). These supracrustal rocks crop out primarily south of Lake Superior in Minnesota, Wisconsin and Michigan, and occur sporadically along the northern and eastern shores of Lake Superior.

In the Terrace Bay area, mafic volcanic rocks of the Osler Group (*circa* 1108 Ma) unconformably overlie the Sibley Group (*circa* 1400 Ma; Davis and Sutcliffe 1985; Heaman and Easton 2006), and 2 groups of volcanic rocks of unknown age, the Coubran Lake and Wolfcamp Lake volcanic rocks (Davis, Hollings and Cundari 2017), unconformably overlie the Coldwell alkalic intrusive complex (*circa* 1108 Ma; Heaman and Machado 1992).

Part 1. Volcanic Stratigraphy of the Western Schreiber–Hemlo Greenstone Belt

INTRODUCTION

The western Schreiber–Hemlo greenstone belt (*see* Figure 1) was the subject of a regional bedrock mapping project during the field seasons of 2015, 2016, 2017 and 2018 (Magnus and Walker 2015; Magnus and Arnold 2016; Magnus 2017b; Magnus and Hastie 2018). This report summarizes the results of this investigation by describing the geochemical characteristics of the volcanic rocks in the greenstone belt, by presenting a stratigraphic model for the greenstone belt and by providing a brief interpretation of the tectonic settings in which the volcanic rocks were generated. The following interpretation is meant to provide a general framework, which more detailed academic studies and mineral exploration programs may refine, adjust and correct.

The Schreiber–Hemlo greenstone belt is among several belts of supracrustal rocks in the Neoarchean Wawa–Abitibi terrane near the north shore of Lake Superior (*see* Figure 1). Magnus (2019c) presents an updated summary of the geological histories and relationships between these greenstone belts. This regional interpretation remains unchanged; however, the availability of additional geochemical and geochronological data (Magnus 2021a, 2021b; Hastie and Magnus 2021a, 2021b) in the western Schreiber–Hemlo greenstone belt has made an update to its genetic model necessary.

SOURCES OF INFORMATION

Four 1:20 000 scale bedrock geology maps generated as part of this project cover the western Schreiber–Hemlo greenstone belt (Magnus 2017a, Magnus 2019a, Magnus 2021a and Hastie and Magnus 2021a). These maps are accompanied by 5 Miscellaneous Release—Data reports that contain field observations, typical rock type photographs and geochemical data (among other data) (Magnus 2018, 2019b, 2021b; Arnold, Hollings and Magnus 2020; Hastie and Magnus 2021b). All geochronological data presented herein (Table 1), whether obtained as part of this project or compiled from published sources, is available in the Geochronology Inventory of Ontario (GeochrON) on the Ontario Geological Survey's OGSEarth webpage.

The maps related to this project (Magnus 2017a, Magnus 2019a, Magnus 2021a; Hastie and Magnus 2021a) depict the bedrock using lithostratigraphic legends in which the metavolcanic rocks are distinguished based on their known or assumed whole-rock major element composition (i.e., mafic, intermediate and felsic metavolcanic rocks), with only partial consideration for their stratigraphic position.

Table 1. List of Archean geochronological data within the boundaries of Figure 2. The "Map Numbers" are also cross-referenced in the stratigraphic interpretation (*see* Figure 8, "corresponding sample" numbers).

Map No.	Age (Ma)	Mineral	Age Interpretation	Rock Class	Stratigraphic Unit	Reference
1	2714	zircon	source population	volcanic	Winston Lake clastic unit	Lodge et al. 2014
1	2685–2740	zircon	source population	volcanic	Winston Lake clastic unit	Lodge et al. 2014
2	2721.2 ± 0.9	zircon	eruption	volcanic	*circa* 2720 Ma volcanic rocks	Lodge et al. 2014
3	2651 ± 6	rutile	cooling	altered	*circa* 2720 Ma volcanic rocks	Davis, Schandl and Wasteneys 1994
3	2672 ± 5	allanite	alteration	altered	*circa* 2720 Ma volcanic rocks	Davis, Schandl and Wasteneys 1994
3	2677 ± 1	monazite	alteration	altered	*circa* 2720 Ma volcanic rocks	Davis, Schandl and Wasteneys 1994
3	2723 ± 2	zircon	eruption	volcanic	*circa* 2720 Ma volcanic rocks	Davis, Schandl and Wasteneys 1994
4	2719 ± 4	zircon	eruption	intrusive	Zenith gabbro	Lodge et al. 2014
5	2717	zircon	source population	volcanic	Winston Lake clastic unit	Lodge et al. 2014
5	2685–2740	zircon	source population	volcanic	Winston Lake clastic unit	Lodge et al. 2014
6	none	NMR		volcanic	Schreiber area volcanic rocks	Davis, Ménard, and Sutcliffe 2018
7	2720.5 ± 3.2	zircon	eruption	volcanic	*circa* 2720 Ma volcanic rocks	Sutcliffe and Davis 2019
8	2677.8 ± 0.9	zircon	emplacement	intrusive	Schreiber pluton	Kamo 2019a
8	2678 ± 1	titanite	emplacement	intrusive	Schreiber pluton	Kamo 2019a
9	2722.6 ± 1.1	zircon	maximum age	intrusive	North Shore occurrence porphyry	Kamo 2019b (2713.2 ± 3.5 Ma) (revised November 2020)
10	2692.1 ± 0.7	zircon	eruption	intrusive	Big Duck Lake pluton	Lodge et al. 2014
10	2700–2716	zircon	inheritance	intrusive	Big Duck Lake pluton	Lodge et al. 2014

Map No.	Age (Ma)	Mineral	Age Interpretation	Rock Class	Stratigraphic Unit	Reference
11	2679 ± 4	zircon	emplacement	intrusive	Longworth Lake pluton	Sutcliffe and Davis 2019
12	none	NMR		volcanic	Schreiber area volcanic rocks	Davis, Ménard and Sutcliffe 2018
13	2698.1 ± 4.5	zircon	emplacement	intrusive	Porphyritic dikes near Schreiber	Sutcliffe and Davis 2019
13	2729–2824	zircon	inheritance	intrusive	Porphyritic dikes near Schreiber	Sutcliffe and Davis 2019
14	2668 ± 31	titanite	metasomatism	intrusive	Syenite Lake pluton	Kamo and Hamilton 2018
14	2682.3 ± 1.1	zircon	emplacement	intrusive	Syenite Lake pluton	Kamo and Hamilton 2018
15	2721.1 ± 4.7	zircon	eruption	volcanic	*circa* 2720 Ma volcanic rocks	Sutcliffe and Davis 2019
16	2636 ± 15	monazite	resetting	intrusive	Crossman Lake batholith	Kamo 2019a
16	2712.8 ± 1.2	zircon	emplacement	intrusive	Crossman Lake batholith	Kamo 2019a
17	2711.4 ± 3.1	zircon	eruption	volcanic		Sutcliffe and Davis 2019
18	2718.5 ± 2.9	zircon	emplacement	volcanic	*circa* 2720 Ma volcanic rocks	Sutcliffe and Davis 2019
19	2677 ± 7	titanite	metamorphism	intrusive	Terrace Bay batholith	Kamo 2016
19	2689 ± 1.1	zircon	emplacement	intrusive	Terrace Bay batholith	Kamo 2016
20	2690.64±0.91	zircon	emplacement	intrusive	Terrace Bay batholith	Kamo and Hamilton 2018
21	none	NMR		intrusive	Lunch Lake pluton	Davis, Ménard and Sutcliffe 2018
22	2667 ± 4	zircon	emplacement	intrusive	Santoy Lake pluton	Kamo 2016
23	2689.3 ± 1.0	zircon	emplacement	intrusive	Steel River pluton	Kamo and Hamilton 2017 (revised June 2021)
24	2720 ± 3	zircon	eruption	volcanic	*circa* 2720 Ma volcanic rocks	Davis and Sutcliffe 2017
25	2676.1 ± 1.3	zircon	emplacement	intrusive	unnamed small pluton	Kamo and Hamilton 2017 (2678 Ma) (revised June 2021)
26	2722 ± 2	zircon	eruption	volcanic	*circa* 2720 Ma volcanic rocks	Davis and Sutcliffe 2017
27	2683 ± 9	zircon	minimum age	volcanic	*circa* 2720 Ma volcanic rocks	Kamo 2016
28	2719 ± 2	zircon	eruption	volcanic	*circa* 2720 Ma volcanic rocks	Davis and Sutcliffe 2017
29	2674 ± 12	titanite	emplacement	intrusive	Foxtrap Lake pluton	Kamo and Hamilton 2018
29	2674.1 ± 1.3	zircon	emplacement	intrusive	Foxtrap Lake pluton	Kamo and Hamilton 2018
30	2684 ± 14	zircon	youngest detrital grain	sedimentary	McKellar Harbour Formation	Davis and Sutcliffe 2017
30	2698 ± 3	zircon	source population	sedimentary	McKellar Harbour Formation	Davis and Sutcliffe 2017
30	2720–2780	zircon	source population	sedimentary	McKellar Harbour Formation	Davis and Sutcliffe 2017
31	2692.8 ± 3.9	zircon	youngest detrital grain	sedimentary	McKellar Harbour Formation	Fralick, Purdon and Davis 2006
31	2693–2793	zircon	source population	sedimentary	McKellar Harbour Formation	Fralick, Purdon and Davis 2006
31	2696.2 ± 2.5	zircon	youngest detrital grain	sedimentary	McKellar Harbour Formation	Fralick, Purdon and Davis 2006
31	2696–2701	zircon	source population	sedimentary	McKellar Harbour Formation	Fralick, Purdon and Davis 2006
31	2735–2778	zircon	source population	sedimentary	McKellar Harbour Formation	Fralick, Purdon and Davis 2006
31	2792.6 ± 1.6	zircon	source population	sedimentary	McKellar Harbour Formation	Fralick, Purdon and Davis 2006
31	2909 ± 1.6	zircon	source population	sedimentary	McKellar Harbour Formation	Fralick, Purdon and Davis 2006
32	2673.4 ± 1.4	zircon	emplacement	intrusive	Little Pic River pluton	Kamo and Hamilton 2017

Abbreviations: *No. = number, NMR = no suitable material recovered, Ma = million years before present.*
Note: *original sample numbers, precise location data, analytical methods and other information can be found in the source references and in the Ontario Geological Survey Geochronology Inventory (Ontario Geological Survey 2019).*

VOLCANIC GEOCHEMISTRY

The western Schreiber–Hemlo greenstone belt, like many greenstone belts in the Superior Province, is composed of a succession of metavolcanic rocks overlain by clastic metasedimentary rocks. These supracrustal rocks are crosscut and surrounded by a variety of synvolcanic, syntectonic and posttectonic plutons. Field observations suggest that the supracrustal rocks in this greenstone belt are generally upright and deformed (ductile shearing and folding) with varied degrees of intensity (Figure 2).

Figure 3 displays the SiO_2 concentrations for all the metavolcanic and clastic metasedimentary rocks sampled and analyzed as part of this project. The metavolcanic samples produce a dominantly "mafic" population that is skewed toward felsic compositions, with a small apparent secondary hump in the higher SiO_2 values. Despite this "bimodal" population, any attempt to split this population into 2 or 3 rock types (mafic and felsic; or mafic, intermediate and felsic) would be arbitrary and potentially misleading. Therefore, trace elements (and petrographic observations) must be considered in order to properly distinguish separate chemostratigraphic units.

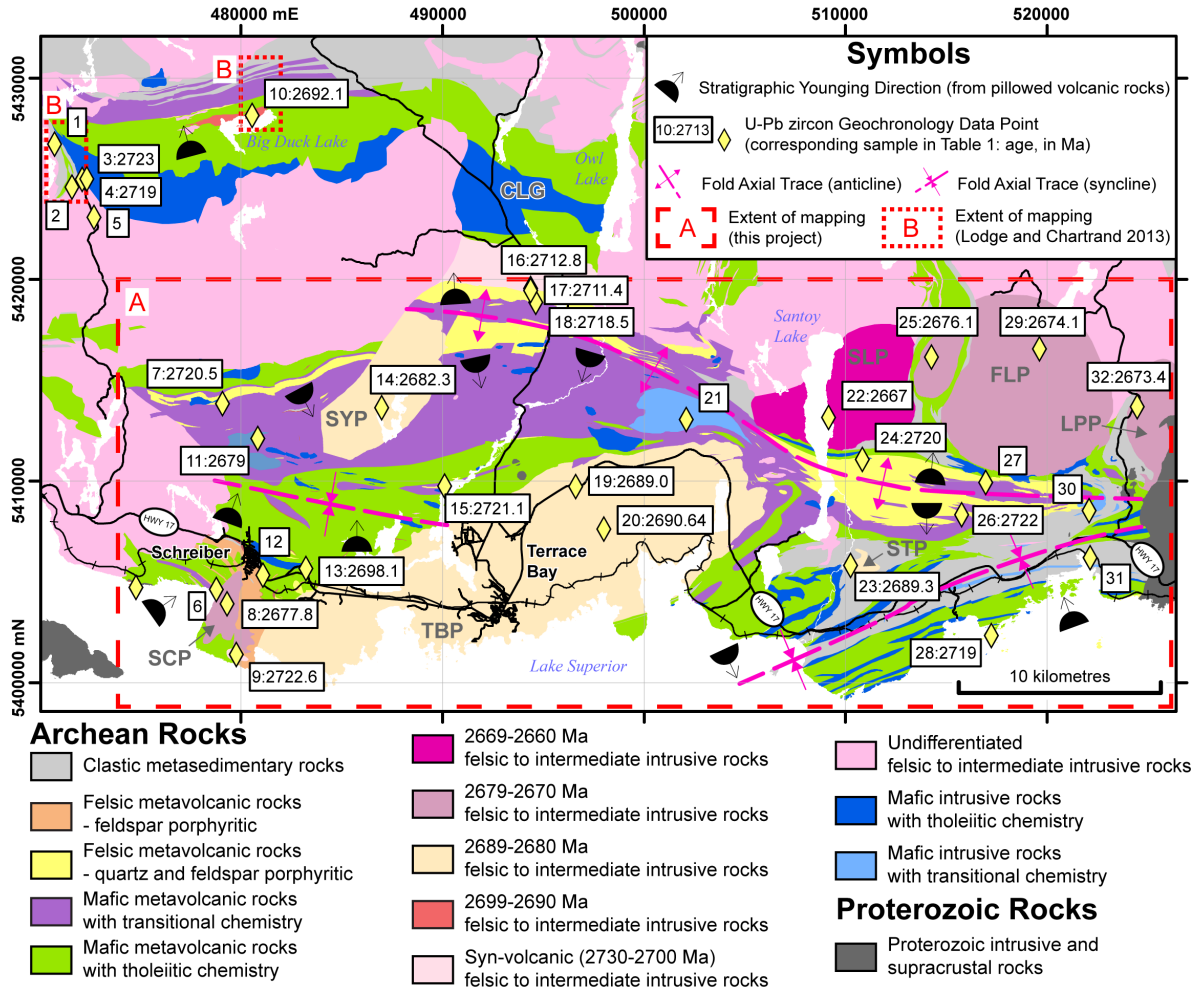

Figure 2. Simplified geological map of the western Schreiber–Hemlo greenstone belt. Abbreviations: CLG, Cameron Lake gabbro: FLP, Foxtrap Lake pluton: LPP, Little Pic River pluton: SCP, Schreiber pluton; SLP, Santoy Lake pluton; STP, Steel River pluton; SYP, Syenite Lake pluton; TBP, Terrace Bay pluton. All geochronological data (numbers 1 to 31) are detailed in Table 1. In the case of sample sites with multiple ages, or detrital ages, or minimum ages, or no material recovered, the ages are not shown on the figure, but are included in Table 1.

The simplified geological map presented herein (*see* Figure 3) distinguishes the metavolcanic rocks based on a combination of their whole-rock major and trace element compositions, resulting in 2 distinct "mafic" metavolcanic rock types and 2 distinct "felsic" metavolcanic rock types. Each of these 4 geochemical rock types correlate with distinct petrographic features and are stratigraphically significant.

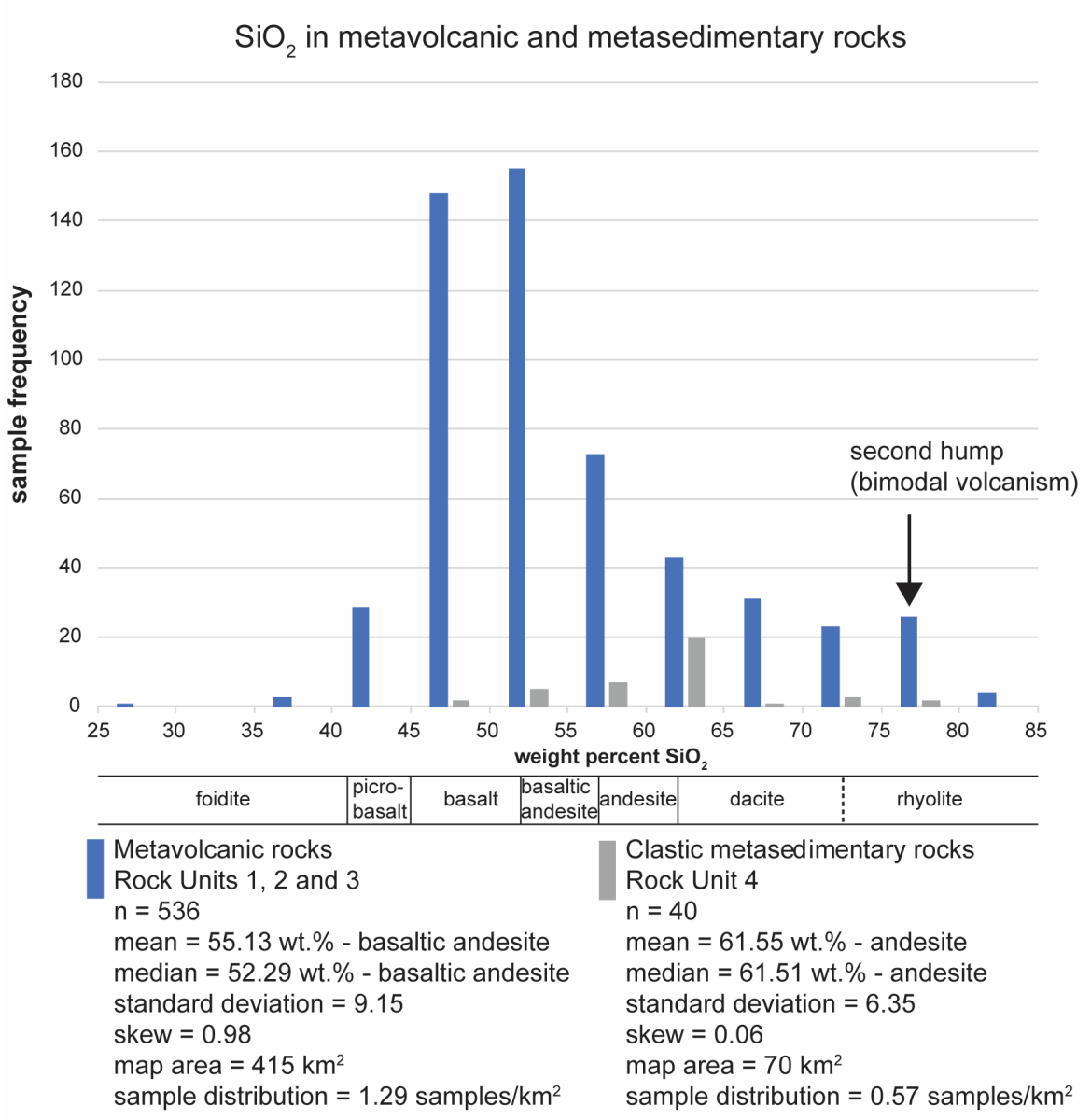

Figure 3. Histogram displaying the SiO_2 concentration in metavolcanic and metasedimentary rocks in the western Schreiber–Hemlo greenstone belt. Volcanic rock classifications corresponding to the Total Alkalis versus Silica diagram (TAS diagram; Le Maitre 1989) are included below the sample frequency diagram. The metavolcanic rocks display a normal distribution around a median composition correlative with "basaltic andesite" and is skewed toward higher SiO_2 values. A slight increase in samples with 75 to 80 wt % SiO_2 suggests that at least 2 populations of volcanic rocks, generated by different volcanic processes, are present in the greenstone belt (i.e., mafic rocks and felsic rocks).

Distinguishing Populations Using Trace Elements

Four chemical groups of metavolcanic rocks are distinguished in the greenstone belt (2 dominantly mafic and 2 dominantly felsic), each with distinct whole-rock major and trace element characteristics, petrographic features and stratigraphic significance. Note that in the subsequent text, the subscript $_{PM}$ indicates that the values are normalized to the primitive mantle values of Sun and McDonough (1995).

The 2 dominantly mafic metavolcanic rock groups were distinguished using a binary diagram that plots Lu-Nd_{PM} vs Th/Nb_{PM}, all normalized to primitive mantle values according to Sun and McDonough (1995) (Figure 4A). The Lu-Nd_{PM} value is meant to represent the slope of the line drawn between heavy rare earth elements (HREEs) on trace element diagrams (Figure 5). More negative slopes are typically interpreted to represent lesser degrees of partial melting in the melt source. The Th/Nb_{PM} value is meant to represent the enrichment of mobile, lithophile elements (such as Th, Pb and light rare earth elements (LREEs)) over generally immobile, high field strength elements (such as Nb, Ta, Ti, Zr and Hf). Greater enrichment of the lithophile elements is typically interpreted to represent greater crustal contamination during volcanogenic processes (such as melting and assimilation) or during postdepositional processes such as hydrothermal alteration. Two distinct populations appear on this diagram which roughly correspond with "tholeiitic" (*see* Figure 5A) and "transitional" (*see* Figure 5B) rocks on a binary discrimination diagram (Ross and Bedard 2009)(*see* Figure 4B). Samples with $Th/Nb_{PM} > 1.8$ are interpreted as contaminated rocks rather than representing a third volcanic population as the Ross and Bedard (2009) discrimination diagram might suggest (*see* Figure 4, field III).

The 2 dominantly felsic metavolcanic rock groups were distinguished based on a single discriminating value: Lu/V_{PM}, which represents a loss of V and several other high field strength elements (Ti and Sc, but not Nb, Ta or Zr) either during melting processes or by fractional crystallization during cooling. The samples with higher Lu/V_{PM} values also appear to have more pronounced loss of phosphorous (*see* Figure 5C). Samples with $Lu/V_{PM} > 10$ have been labelled as "highly fractionated rocks" (*see* Figure 5C), and those with $Lu/V_{PM} < 10$ are part of a more nondistinct, geochemically ambiguous population (*see* Figure 5D).

Trace element diagrams for each of these 4 populations are illustrated in Figure 5 to help visualize their individual characteristics. Trace element diagrams displaying average values (sheathed by 1st and 3rd quartile values) are displayed in Figure 6 to help visualize the contrasts between the 2 dominantly mafic (*see* Figure 6A) and the 2 dominantly felsic populations (*see* Figure 6B). Histograms for the SiO_2 content of each population are displayed in Figure 7 to help visualize and compare the behavior of major elements within these volcanic rock types.

The distribution of these volcanic rock types is illustrated on the simplified geological map (*see* Figure 2) and in the simplified stratigraphic column (*see* Figure 8).

Tholeiitic Mafic to Intermediate Metavolcanic Rocks

Trace element patterns for the tholeiitic rocks (*see* Figure 5A) are similar to the global average value for mid-ocean ridge basalt (MORB, Averalo and McDonough 2010), with several small deviations. The tholeiitic rocks are slightly depleted in P and Ti, which suggests that the mineral apatite is stable in the melt source, and they are slightly enriched in Th, which suggests that the melt source has been slightly contaminated by crustal components.

On an SiO_2 (wt %) histogram (*see* Figure 7), the tholeiitic rocks produce a normal distribution heavily concentrated around an average of 50.5 wt % SiO_2 (basalt), with minor dispersion into higher and

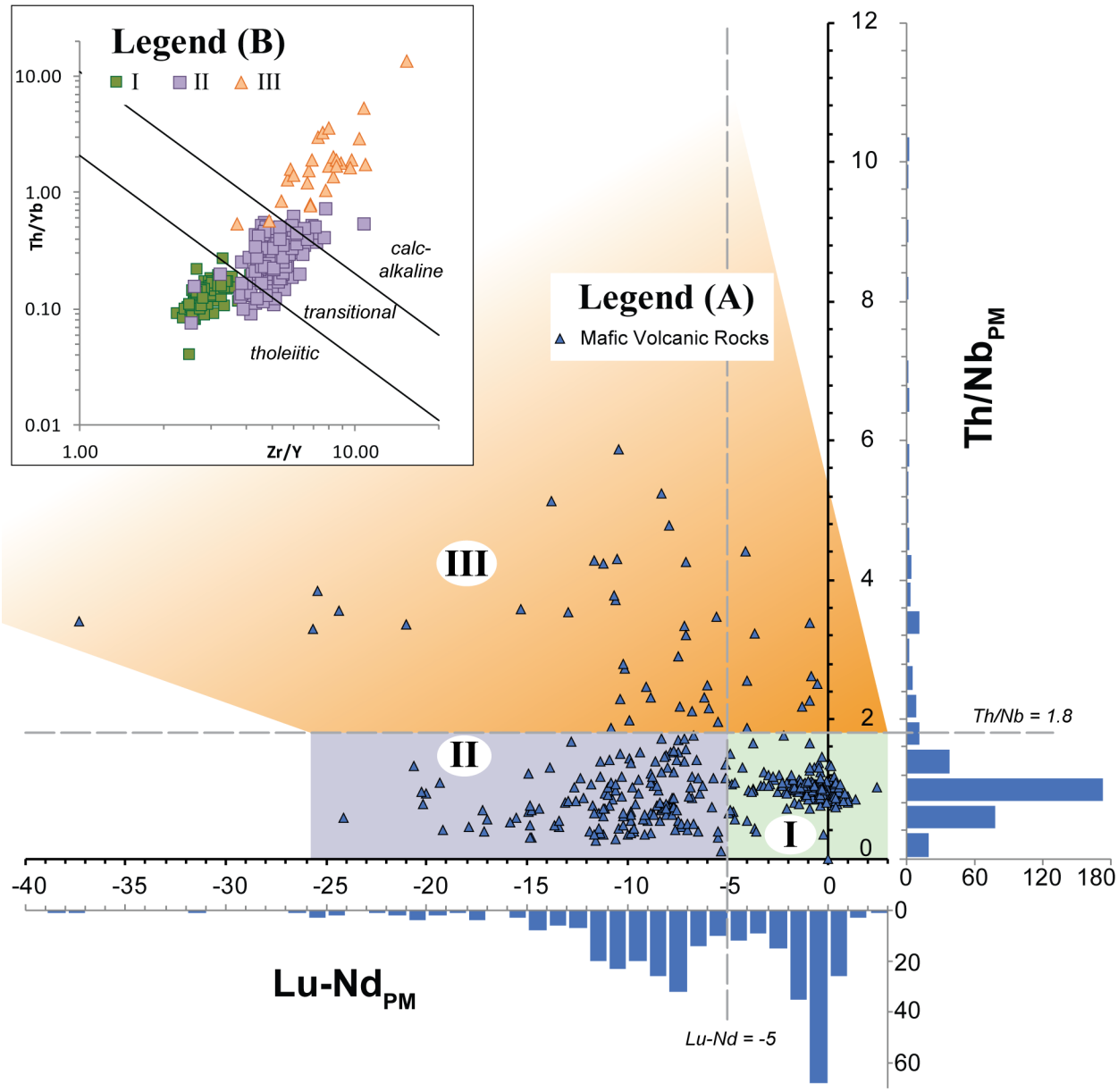

Figure 4. **A)** Binary plot of Lu-Nd versus Th/Nb, all values normalized to Primitive Mantle values (Sun and McDonough 1995). Lu-Nd is meant to represent the slope of the heavy rare earth elements as viewed on trace element diagrams (*see* Figures 5 and 6); more negative slopes are generally correlative with lower degrees of partial melting. Th/Nb is meant to represent the enrichment of Th over Nb; higher concentrations of Th are generally correlative with greater crustal contamination or metasomatism. Histograms are presented along both axes to help illustrate the division between observed sample populations. Two populations are apparent along the X-axis; thus, they have been split at a value between the 2 peaks (Lu-Nd = -5). One population with abundant outliers is apparent along the Y-axis. The samples have been separated from the outliers at a value of Th/Nb = 1.8, below which the samples produce a nearly normal population. In two-dimensional space, the samples of mafic rocks produce 2 clusters—fields I and II—and appear to deviate from these clusters variably into field III. Therefore, the clusters in fields I and II are believed to represent real metavolcanic populations, and the samples in field III are interpreted to represent contaminated or metasomatized samples. **B)** Binary plot of Th/Yb versus Zr/Y meant to discriminate between tholeiitic, transitional and calc-alkaline mafic rocks (Ross and Bedard 2009). Samples from fields I, II and III on plot A generally correlate with the tholeiitic, transitional and calc-alkaline fields, respectively, with some overlap between populations. Therefore, the samples from fields I and II are interpreted to have "tholeiitic" and "transitional" chemistry, respectively, and the samples from field III are considered to represent a false population consisting of altered samples from the other 2 populations.

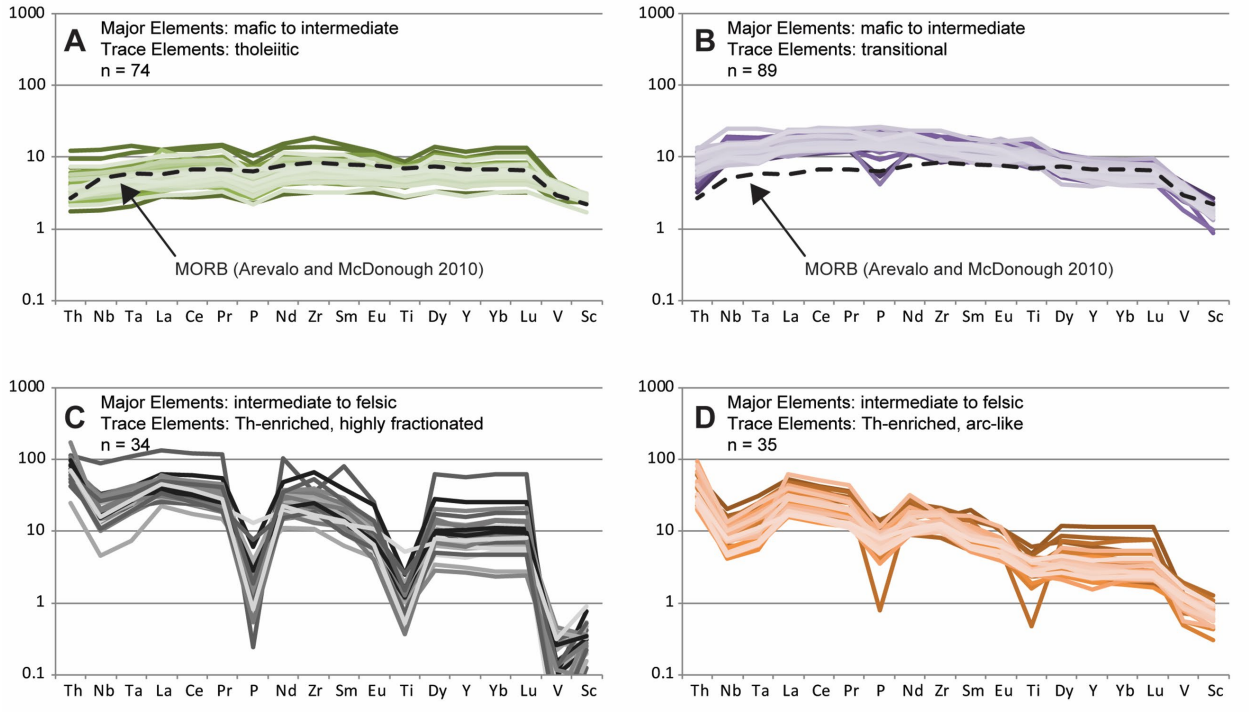

Figure 5. Trace element diagrams normalized to Primitive Mantle (PM) values (Sun and McDonough 1995). **A)** Samples of mafic (basalt and basaltic andesite) rocks with tholeiitic trace element concentrations, overlain by a dashed line depicting the trace element concentrations of global mid-ocean ridge basalt (MORB, Averalo and McDonough 2010). **B)** samples of mafic rocks with trace element concentrations transitional between "tholeiitic" and "calc-alkalic", overlain by a dashed line depicting the trace element concentrations of global mid-ocean ridge basalt (MORB, Averalo and McDonough 2010). In both A and B, only mafic samples with Th/Nb < 1 have been displayed, to reduce clutter and to help represent the least contaminated samples. **C)** Samples of dacitic and rhyolitic rocks with distinct highly fractionated heavy rare earth element concentrations, discriminated by Lu/V > 10 (PM-normalized). **D)** Samples of dacitic and rhyolitic rocks with Lu/V < 10. This negatively sloping pattern with moderately fractionated P, Ti and heavy REEs and enriched Th is commonly associated with "calc-alkalic" rocks generated in volcanic arc environments. This pattern is common among several other rock types in the greenstone belt, including clastic metasedimentary rocks, altered mafic to intermediate metavolcanic rocks and intermediate to felsic granitoid rocks.

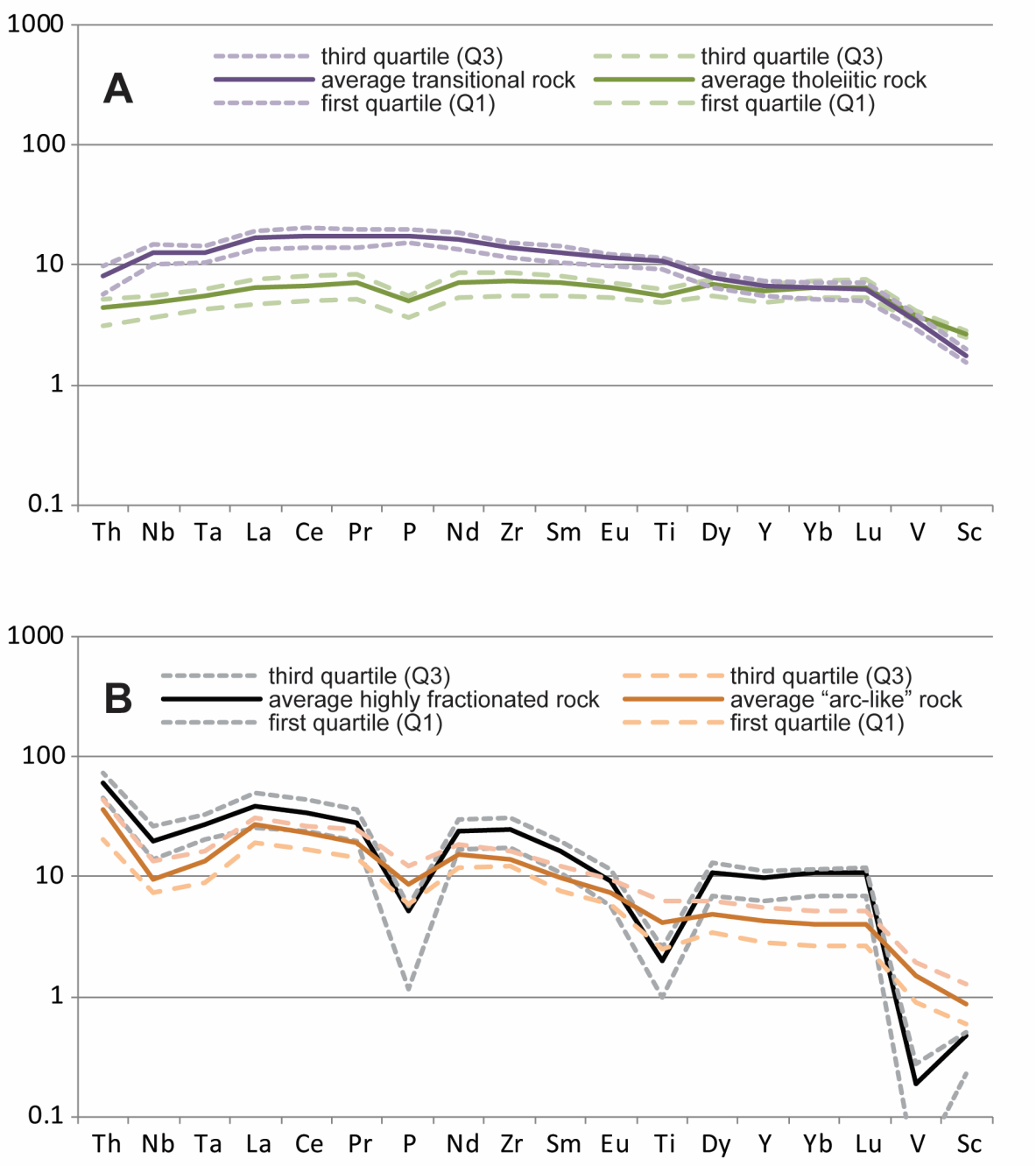

Figure 6. Trace element diagrams normalized to Primitive Mantle values (Sun and McDonough 1995) displaying averages for **A)** mafic to intermediate rocks (basalt, basaltic andesite and andesite) with tholeiitic (80 samples) and transitional (100 samples) trace element concentrations and **B)** intermediate to felsic rocks (andesite, dacite and rhyolite) with highly fractionated (58 samples) and less-fractionated (average "arc-like" (67 samples)) trace element concentrations. Averages are represented by solid lines; dashed lines below and above the averages represent the first and third quartile values, below and above the averages, respectively.

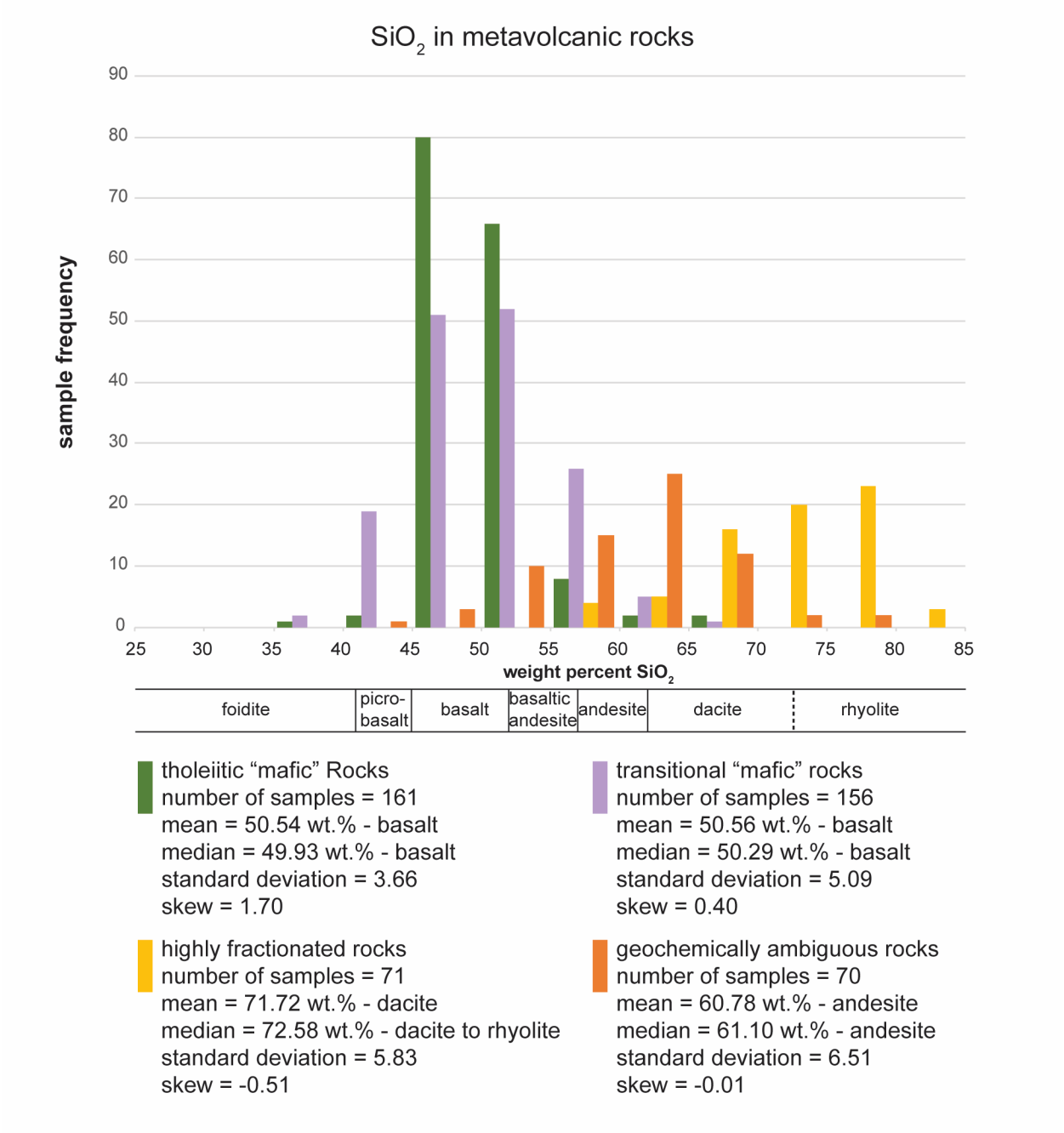

Figure 7. Histogram displaying SiO_2 concentration in the 3 distinct geochemical populations identified in the greenstone belt, as well as the population of "geochemically ambiguous rocks" that include volcaniclastic rocks and altered "mafic, intermediate and felsic" rocks. It is important to note that these "geochemically ambiguous" rocks display a similar distribution to the clastic sedimentary rocks illustrated in Figure 3. The 4 populations depicted here are mutually exclusive.

lower SiO_2 values. The narrow range for SiO_2 values suggests that minimal fractional crystallization occurred during cooling, which is an indication that the melts spent very little time in the crust prior to eruption and cooling. Sparse occurrences of more ultramafic and more felsic rocks likely represent fractional crystallization at a local scale, possibly caused by local physical or chemical traps.

Petrographically, the rocks with tholeiitic chemistry correlate with massive to pillowed mafic flows, both with and without variolitic textures. The variolitic flows in this greenstone belt all correlate with the tholeiitic geochemical group, which makes them a useful tool for identifying geochemical rock types in this greenstone belt. However, it is uncertain whether their variolitic texture is directly related to their tholeiitic chemistry. It is possible that variolitic textures can occur in mafic rocks with transitional, calc-alkalic or even alkalic geochemistry, and therefore the use of variolitic flows as a geochemical field mapping tool must be investigated for their utility in each individual greenstone belt where they are found to occur. The occurrences of tholeiitic rocks without varioles remain ambiguous without geochemical analysis. Local occurrences of cumulate rocks and spinifex-like textures are associated with more ultramafic tholeiitic rocks.

Transitional Mafic to Intermediate Metavolcanic Rocks

Trace element patterns for the transitional rocks (*see* Figure 5B) present an overall concave downward curved pattern. The transitional rocks are depleted in Th, which suggests that their mantle source had not been contaminated by crustal components, unlike the tholeiitic rocks. These rocks are more enriched in LREEs and more depleted in HREEs, which is typically associated with lower degrees of partial melting. Phosphorous displays both small positive and negative anomalies, which suggests that apatite was affected by fractional crystallization prior to eruption.

On an SiO_2 (wt %) histogram (*see* Figure 7), the transitional rocks show a normal distribution with an average of 50.6 wt % SiO_2 (basalt), but with broader "shoulders" than the tholeiitic rocks. This wider range of compositions suggests that the magma that formed these rocks experienced fractional crystallization prior to eruption, which requires residence in a magma chamber or other, more complicated, crustal plumbing features.

Petrographically, the rocks with transitional chemistry correlate with massive to pillowed mafic to intermediate flows, commonly with abundant coarse-grained plagioclase phenocrysts and amygdules, although in some cases the observed flows had no distinct petrographic characteristics. The abundance of plagioclase phenocrysts supports the geochemical observations that fractional crystallization occurred prior to eruption, potentially in a magma chamber. However, plagioclase fractionation is commonly associated with variable Eu anomalies, which were not observed. Europium fractionation concomitant with plagioclase fractionation typically occurs in magmas that have been oxidized, which cause Eu^{2+} to oxidize to Eu^{3+}. The absence of this geochemical feature suggests that the parent magma was under reducing conditions, which supports the earlier observation that the melt source was likely not contaminated by crustal components (which are typically introduced to the mantle by oxidizing, hydrated fluids that transport Th and other mobile elements from subducted components; e.g., Plank 2005).

The significance of the abundance of coarse amygdules is difficult to interpret because of the myriad of environmental and magmatic conditions that can affect the appearance, abundance and size of amygdules. Nonetheless, the abundant, coarse amygdules (and plagioclase phenocrysts), when observed, can be used as a field-marker for this geochemical group in this greenstone belt.

Highly Fractionated Felsic Metavolcanic Rocks

This group of "highly fractionated rocks" is defined by its highly fractionated trace element patterns (*see* Figure 5C) in contrast with felsic to intermediate rocks with less significantly fractionated patterns (*see* Figure 6B). The highly fractionated rocks have significant negative P, Ti, V and Sc anomalies. Other high field strength elements, such as Nb, Ta and Zr, appear not to have been significantly fractionated. These rocks also tend to have flatter trace element patterns than the less fractionated felsic rocks (*see* Figure 6B). It is unclear whether the shallower slope of the trace element patterns and the severity of their fractionated anomalies are related, and it is unclear whether these characteristics are related to the conditions present in their melt sources, fractional crystallization processes or postdepositional processes.

On an SiO_2 (wt %) histogram (*see* Figure 7), the highly fractionated rocks produce a normal distribution with a pronounced negative skew, making the distribution look almost wedge-shaped. This may appear to indicate that rocks with higher SiO_2 concentration would have higher degrees of fractionation; however, there is no correlation between SiO_2 and Lu/V_{PM}. The lack of correlation indicates that the processes that produce the quartz phenocrysts (described below), and those that produce the highly fractionated trace element patterns, are overlapping processes that operate independently.

Petrographically, these highly fractionated, silica-rich rocks correlate with quartz and feldspar porphyritic felsic volcanic and volcaniclastic rocks. These occur mainly as volcaniclastic and epiclastic rocks such as tuffs, tuff breccias, volcanic conglomerates and volcanic wackes, with very few confirmed occurrences of coherent flows (i.e., lava domes). Because of the partly magmatic, partly sedimentary nature of these volcaniclastic rocks, their geochemistry is likely to have been influenced by sedimentary, hydrothermal and metamorphic processes, all of which can mobilize crustal (lithophile) elements, making an interpretation of these patterns in an igneous context difficult.

Geochemically Ambiguous Intermediate Metavolcanic Rocks

There are a variety of rocks in this greenstone belt that display similar trace element patterns to this fourth, geochemically ambiguous population, including altered varieties of both tholeiitic and transitional mafic volcanic and intrusive rocks, interflow volcaniclastic rocks, quartz porphyritic felsic volcanic and intrusive rocks (without the highly fractionated signature), alkalic mafic porphyritic dikes, granitoid rocks and a majority of the clastic metasedimentary rocks sampled in the McKellar Harbour Formation. The wide variety of rock types that have been identified with this geochemical signature precludes this signature being used as a diagnostic feature, and so identification of rocks in this population heavily depends on field and petrographic observations. The samples included in the geochemical figures in this report for this population include only those samples that have been positively identified as volcanic or volcaniclastic in origin.

Samples in this population have trace element patterns that are generally enriched in Th over Nb, enriched in LREEs over HREEs, and display slightly negative P and Ti anomalies (*see* Figure 5D), and are distinguished from the highly fractionated rocks by their $Lu/V_{PM} < 10$ and more inclined trace element pattern (*see* Figure 6B). In primary magmatic rocks, this geochemical signature is typically attributed to contamination by crustal components either in the mantle during melting, during ascent of the magma through the crust, or during residence in a magma chamber in the crust. As with the highly fractionated rocks, the volcaniclastic rocks with this pattern can also have been influenced by sedimentary, hydrothermal and metamorphic processes, all of which can mobilize crustal (lithophile) elements, making an interpretation of these patterns difficult.

On an SiO_2 (wt %) histogram (*see* Figure 7), this population produces a normal distribution around an average of 60.8 wt % SiO_2. This population and its statistics are very similar to those of the clastic sedimentary rocks collected from the McKellar Harbour Formation, displayed in Figure 3. Although not displayed here, the concentrations of other major and trace elements are likewise similar between these volcaniclastic rocks and the clastic sedimentary rocks of the McKellar Harbour Formation. Thus, distinction of this volcaniclastic unit relies heavily upon field and petrographic observations.

Petrographically, these rocks are feldspar porphyritic (and less commonly also quartz porphyritic) volcanic and volcaniclastic rocks, including tuffs, tuff breccias, volcanic conglomerates and volcanic wackes.

VOLCANIC STRATIGRAPHY

The lower part of the stratigraphy in the western Schreiber–Hemlo greenstone belt is split into 2 parts (Figure 8). The volcanic rocks south of the town of Schreiber (part 1) and the older sequence of volcanic rocks in the remainder of the greenstone belt (part 2) are interpreted to have formed in separate (but potentially adjacent and overlapping) depositional environments. Both of these older sequences were then overlain by the younger volcanic and sedimentary rocks of the upper part of the stratigraphy.

Older Stratigraphy

The oldest rocks in the stratigraphy in the greenstone belt are tholeiitic mafic metavolcanic rocks that extend from the Big Duck Lake area toward Owl Lake and occur in a thin sliver of bedrock west of the Syenite Lake pluton (*see* Figure 2). These rocks are overlain by a starved succession (*see* Figure 8, st.s. I) composed of chert and other chemical metasedimentary rocks. This older stratigraphy and the starved succession have been inferred based on relatively few geochemical samples and sparse field observations; more detailed mapping in the Big Duck Lake and Owl Lake areas is required to better understand the nature of volcanism and the transition between the volcanic rocks at this interval.

Starved Succession I is overlain by a sequence of interbedded transitional mafic metavolcanic rocks (with abundant plagioclase phenocrysts and amygdules) and both highly fractionated and less fractionated felsic volcaniclastic rocks (both with and without quartz phenocrysts). The metavolcanic rocks in this sequence are interpreted to have spent some time residing in the crust prior to eruption, likely in magma chambers, based on the major and trace element characteristics of the transitional mafic rocks and the appearance of abundant phenocrysts in both the mafic and felsic metavolcanic rocks. The formation of magma chambers and greater degrees of magmatic evolution are typically associated with crustal thickening processes, either by compressional tectonism (arc volcanism) or mantle plume-influenced volcanism.

The plagioclase porphyritic, geochemically ambiguous felsic volcaniclastic rocks (without quartz phenocrysts) in this part of the stratigraphy may represent reworked volcaniclastic material from the slightly older volcano in the Schreiber area (described below). It is interpreted that this part of the stratigraphy represents a depositional basin into which 3 components were deposited:

- Transitional mafic metavolcanic rocks, erupted directly into the basin
  - Massive to pillowed flows with abundant plagioclase phenocrysts and amygdules
- Feldspar porphyritic felsic volcaniclastic rocks, scavenged from the volcanic centre near Schreiber
  - Fine-grained tuffaceous rocks with only feldspar phenocrysts
- Quartz and feldspar porphyritic felsic volcanic and volcaniclastic rocks, erupted directly into the basin and proximally reworked
  - Coherent flows; coarse volcaniclastic rocks including tuff breccias and volcanic conglomerates

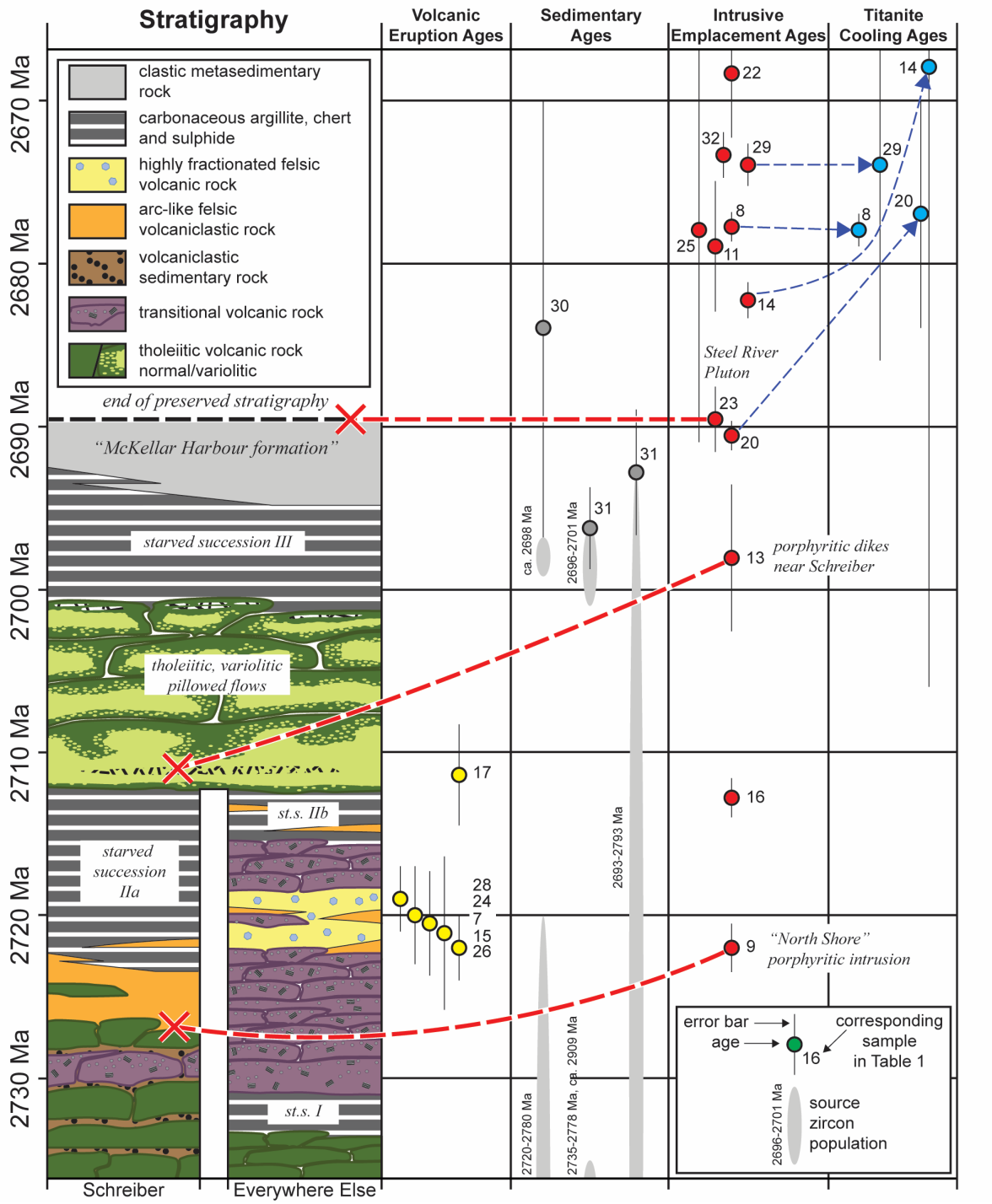

Figure 8. Simplified stratigraphic column for the western Schreiber–Hemlo greenstone belt with geochronology data (*see* Table 1 for details). The lower part of the stratigraphy is split into 2 parts: 1) volcanic rocks south of the town of Schreiber, and 2) the older sequence of volcanic rocks in the remainder of the greenstone belt. In many cases, the chronological placement of contacts between units is uncertain, and therefore this should be interpreted as a relative stratigraphic column. The most robust constraint in this stratigraphy is the package of *circa* 2720 Ma quartz porphyritic, highly fractionated felsic metavolcanic rocks observed throughout the greenstone belt. Ages for volcanic, sedimentary and intrusive rocks are based on zircon. Red X symbols indicate the estimated place in the stratigraphy that their connected intrusive rocks crosscut, providing minimum age constraints for those places in the stratigraphy. Note: the closing temperature for zircon is roughly 900°C and for titanite is 650 to 500°C, the latter roughly corresponding to lower amphibolite facies metamorphic conditions. Abbreviations: ca., *circa;* Ma, million years before present; st.s., starved succession.

The quartz porphyritic felsic metavolcanic rocks contain abundant zircons suitable for geochronological analysis and have produced consistent U/Pb zircon ages of *circa* 2720 Ma (*see* Figure 2, geochronology points 7, 15, 18, 24, 26 and 28). This stratigraphic horizon has provided the most confident geochronological marker against which the remainder of the stratigraphy has been relatively adjusted. This stratigraphic horizon is significant because metavolcanic rocks *circa* 2720 Ma in age are associated with volcanogenic massive sulphide mineralization at Winston Lake (*see* Figure 2, geochronology points 1 to 5), in the nearby Manitouwadge and Shebandowan greenstone belts (*see* Figure 1), and in the Kidd–Munro assemblage in the Abitibi greenstone belt of the eastern Wawa–Abitibi terrane.

Two ages at *circa* 2710 Ma have been obtained from adjacent felsic intrusive and felsic metavolcanic rocks along the northern edge of the greenstone belt (*see* Figure 2, geochronology points 16 and 17). Two preliminary interpretations of these data include the following:

- Extending the entire sequence of associated transitional mafic volcanic rocks and variably fractionated and porphyritic felsic volcanic rocks from *circa* 2720 Ma to *circa* 2710 Ma. This would compress the stratigraphic units above these rocks in the stratigraphy.

- Adding a distinct metavolcanic event at *circa* 2710 Ma to the stratigraphy that occurs only in this locality, perhaps concurrently with some of the other younger stratigraphic units.

More detailed mapping and sampling in both the granitoid and metavolcanic rocks along this edge of the greenstone belt is required to better establish these ages and understand their significance.

Starved Succession IIb, which is composed of chert, carbonaceous argillite, sulphide facies iron formation and felsic tuffaceous rocks, marks the contact between transitional and variolitic tholeiitic mafic rocks across the entire western Schreiber–Hemlo greenstone belt. Starved Succession IIb is spatially associated with a variety of gold and base metal occurrences, including the historic Empress Mine in Syine Township, where these rocks are isoclinally folded (*see* Magnus 2017b, 2019a). This succession is believed to be synchronous with the later part of Starved Succession IIa; however, the relationship between these rocks is obscured by the overlying metavolcanic rocks. Nonetheless, the stratigraphy for the entire western Schreiber–Hemlo greenstone belt is merged following Starved Succession II.

Older Stratigraphy, Schreiber Area

The oldest rocks in the stratigraphy south of the town of Schreiber are massive to pillowed tholeiitic mafic rocks, best observed along the shores of Lake Superior west of Schreiber Beach. Volcanic conglomerates, wackes and siltstones are commonly observed between the mafic flows in this sequence. The abundance and variety of clastic rocks between flows indicates a locally high-relief depositional environment, such as along the flanks of a stratovolcano or volcanic island.

One flow has transitional trace element characteristics similar to the transitional mafic rocks (*circa* 2720 Ma) elsewhere in the greenstone belt, which may indicate that the rocks near Schreiber and those in the remainder of the greenstone belt were deposited in overlapping or contiguous volcanic environments.

The sequence of mafic rocks is overlain by an interval of feldspar porphyritic volcaniclastic rocks, predominantly tuff breccias and volcanic conglomerates. These rocks have ambiguous trace element geochemistry; there have been no felsic rocks observed with either quartz phenocrysts or highly fractionated trace element characteristics. The coarse and homogenous nature of these volcaniclastic

rocks indicate a close proximity to their volcanic source; however, no coherent flows or equivalent intrusive rocks have been identified, so the precise location of the volcanic centre is unknown.

The top of this sequence is marked by a starved succession (*see* Figure 8, starved succession IIa) composed of carbonaceous argillites and cherts, which are best observed along Highway 17 west of the town of Schreiber. There are sparse volcaniclastic beds at the bottom of this succession which likely represent sedimentary reworking of the underlying volcaniclastic pile.

Despite several sampling attempts, no zircons have been retrieved from this part of the stratigraphy for geochronological analysis. A quartz and feldspar porphyritic felsic intrusion crosscuts this stratigraphy at the North Shore gold occurrence (*see* Figure 2, geochronology point 9), placing a minimum age constraint on this stratigraphy at *circa* 2720 Ma.

Younger, Merged Stratigraphy

A homogenous succession of tholeiitic mafic metavolcanic rocks overlie Starved Succession IIa and IIb across the entire greenstone belt, with very few occurrences of clastic sedimentary rocks or felsic metavolcanic rocks occurring in this part of the stratigraphy. These rocks occur as massive to pillowed flows and commonly display distinct variolitic textures that have not been observed in any other part of the stratigraphy. These rocks are more thoroughly described in Magnus (2017b, 2019c).

Based on the geochemical characteristics of these rocks and the absence of plagioclase phenocrysts, these rocks did not undergo significant fractional crystallization prior to eruption, which indicates that the parent magmas spent very little time in the crust before eruption. This is consistent with an extensional volcanic depositional environment, where the crust is becoming thinner and magmatic plumbing systems open more readily than in compressional environments. The slight enrichment in Th compared to mid-ocean ridge basalt (MORB) suggests that crustal components were added to the mantle source for these rocks prior to melting. This is typically attributed to mantle metasomatism during subduction in a volcanic arc environment (Plank 2005). This arc-related geochemical signature, combined with the interpreted extensional volcanic environment, are consistent with a back-arc basin depositional environment.

A quartz and feldspar porphyritic dike that crosscuts these rocks near the town of Schreiber has a U/Pb zircon age of 2698.1±4.5 Ma (*see* Figure 2, geochronology point 13; Sutcliffe and Davis 2019), constraining the deposition of these rocks to a minimum age of *circa* 2700 Ma. A more detailed investigation of the sparse felsic metavolcanic rocks that are interbedded with these rocks may provide better constraints on the timing of deposition for the tholeiitic mafic rocks.

Based on compiled data, these variolitic, tholeiitic rocks do not exist in the Big Duck Lake area and their presence in the Owl Lake area has yet to be confirmed; more detailed mapping in these areas is required to better understand this part of the stratigraphy to the north (*see* Figure 2).

East of the Terrace Bay Pluton (*see* Figure 2), the variolitic, tholeiitic rocks are overlain by Starved Succession III, which is composed of chert and carbonaceous argillite with minor sulphide facies iron formation. At the top of this succession, these rocks become progressively interbedded and eventually overwhelmed by turbiditic wackes of the McKellar Harbour Formation. These sedimentary rocks have been interpreted to represent down-slope equivalents of the clastic sedimentary rocks of the Quetico Terrane to the north (Fralick, Purdon and Davis 2006).

Some of the youngest zircons in these rocks range from *circa* 2696–2690 Ma (*see* Figure 8, geochronology points 30 and 31) and may have been derived from synchronous volcanism documented in

the Hemlo area of the eastern Schreiber–Hemlo greenstone belt and in the Shebandowan greenstone belt (*see* Magnus 2019c and references therein). The Steel River pluton, with a U/Pb age of 2689.3±1.0 Ma (*see* Figure 2, geochronology point 23), crosscuts the McKellar Harbour Formation, constraining the deposition of the formation to a minimum age of *circa* 2690 Ma. This is extremely close in age to the maximum age of deposition (*circa* 2696–2690 Ma) for the McKellar Harbour Formation; additional detailed mapping and geochronological sampling of the McKellar Harbour Formation, the Steel River pluton and other Archean intrusive rocks that crosscut the formation is required to better understand the timing and relationship between these rock units.

In the Big Duck Lake area, it appears as though transitional mafic metavolcanic rocks (*circa* 2720 Ma) are directly overlain by Starved Succession III and clastic metasedimentary rocks of the Quetico terrane; however, additional detailed mapping and sampling is required to better understand the stratigraphy in that area.

POSTDEPOSITIONAL GEOCHRONOLOGY

Felsic to intermediate intrusive rocks that crosscut and surround the supracrustal rocks of the western Schreiber Hemlo greenstone belt range in age from *circa* 2690 Ma (Terrace Bay and Steel River plutons) to 2667±4 Ma (Santoy Lake pluton, *see* Figure 2). Several observations have been made related to the geochronology and morphology of these intrusive rocks that have implications for the history of regional deformation and metamorphism (*see* Figures 2 and 8).

- Intrusions emplaced prior to *circa* 2680 Ma tend to be oblong or irregular in morphology and tend to be oriented subparallel to the regional foliation in the greenstone belt (striking generally east-northeast). These include the Terrace Bay, Steel River and Syenite Lake plutons, and a felsic porphyritic intrusion in the Big Duck Lake area.
    - Titanite cooling ages for these plutons are all younger than *circa* 2680 Ma, significantly younger than the emplacement ages for the plutons.
- Intrusions emplaced after *circa* 2680 Ma tend to be equant and round in morphology, and because of their equant aspect ratios, do not have a discernable orientation. These include the Little Pic River, Foxtrap Lake and Santoy Lake plutons and a small unnamed pluton between the latter two.
    - Titanite cooling ages for these plutons are very close to the emplacement ages for the plutons (younger than *circa* 2680 Ma).

Although the timing of the initiation of regional deformation is still unclear, since the sequence of tholeiitic mafic metavolcanic rocks were likely erupted in an extensional tectonic environment, this provides a maximum age of *circa* 2700 Ma for the onset of regional compressional tectonism.

The above listed observations indicate that prior to *circa* 2680 Ma, regional deformation caused the development of regional-scale structural fabrics, affected the shape and orientation of major intrusive rocks, and maintained a regional temperature of at least ~660°C (closing temperature for titanite; Scott and St-Onge 1995), equivalent to upper amphibolite facies metamorphism. This is consistent with amphibolite facies metamorphic mineral assemblages observed in deformed rocks throughout the greenstone belt. Rocks with poorly developed structural fabrics and greenschist facies mineral assemblages (which have been observed locally in the greenstone belt) are assumed to represent metastable assemblages and should not be used to infer metamorphic gradients.

After *circa* 2680 Ma, the intensity of regional deformation decreased, lowering the regional temperature and ceasing to affect the emplacement and shape of major plutons. Any deformed rocks in the greenstone belt with greenschist facies mineral assemblages are assumed to have been deformed under lower pressure and temperature conditions after *circa* 2680 Ma.

These inferences have been made based on a limited number of titanite ages. To further constrain the timing of regional deformational events, more detailed analysis of pressure and temperature sensitive minerals in a greater variety of both plutonic and supracrustal rocks is required.

WHOLE ROCK ISOTOPE GEOCHEMISTRY

Twenty-six samples of metavolcanic rocks and 13 samples of granitoid rocks were analyzed for Sm-Nd isotopic systematics as part of this project (Magnus 2021b). The metavolcanic samples include representative samples from each major part of the stratigraphy and include representative samples of each of the geochemical populations discussed herein.

Epsilon Nd values at 2700 Ma (εNd_{2700}) for most of the metavolcanic samples are between +1 and +3 ε_{Nd} units and are generally within error (estimated at ±0.3 epsilon units) of the depleted mantle value at 2700 Ma (Figure 9). These data indicate that the mafic metavolcanic rocks throughout the stratigraphy were derived from isotopically unaltered depleted mantle sources. The felsic metavolcanic rocks have similar ε_{Nd} values near the depleted mantle value. This indicates that they were generated by melting of very young (juvenile) mafic components either in the lower crust or young mafic components in the mantle (such as subducted oceanic crust).

In more mature volcanic settings with older crustal components, ε_{Nd} values for mafic and felsic volcanic rocks are typically shifted toward more negative values, below the depleted mantle value (Dickin 2018). Several metavolcanic samples in this data set have ε_{Nd} values significantly above the depleted mantle value (*see* Figure 9). To generate these higher values naturally in a volcanic setting, the rocks would have to have been derived from a mantle source that separated from the bulk earth earlier than the depleted mantle presumably did. It is more likely that these higher values can be attributed to unpredictable isotopic fractionation during postdepositional processes such as hydrothermal alteration.

Epsilon Nd values for the granitoid rocks are likewise clustered around the depleted mantle value at the time of emplacement (Magnus 2021b), which indicates that significantly older crustal components were absent from their melt sources during and after regional tectonism.

GEOLOGICAL HISTORY AND TECTONIC SETTINGS

The stratigraphy of the western Schreiber–Hemlo greenstone belt preserves evidence of several types of mafic and felsic volcanism over a span of at least 20 million years. This includes 2 distinct and likely overlapping volcanic depositional environments that developed on top of tholeiitic oceanic crust (prior to and at *circa* 2720 Ma) that were later overlain by another thick, homogenous sequence of tholeiitic mafic rocks that developed in a back-arc tectonic environment. Volcanism in this greenstone belt ceased by *circa* 2700 Ma; however, the overlying clastic metasedimentary rocks of the McKellar Harbour Formation incorporated zircons *circa* 2700–2690 Ma in age that were likely derived from ongoing felsic volcanism in the nearby eastern Schreiber–Hemlo and Shebandowan greenstone belts, which are presumed to be part of the same depositional setting.

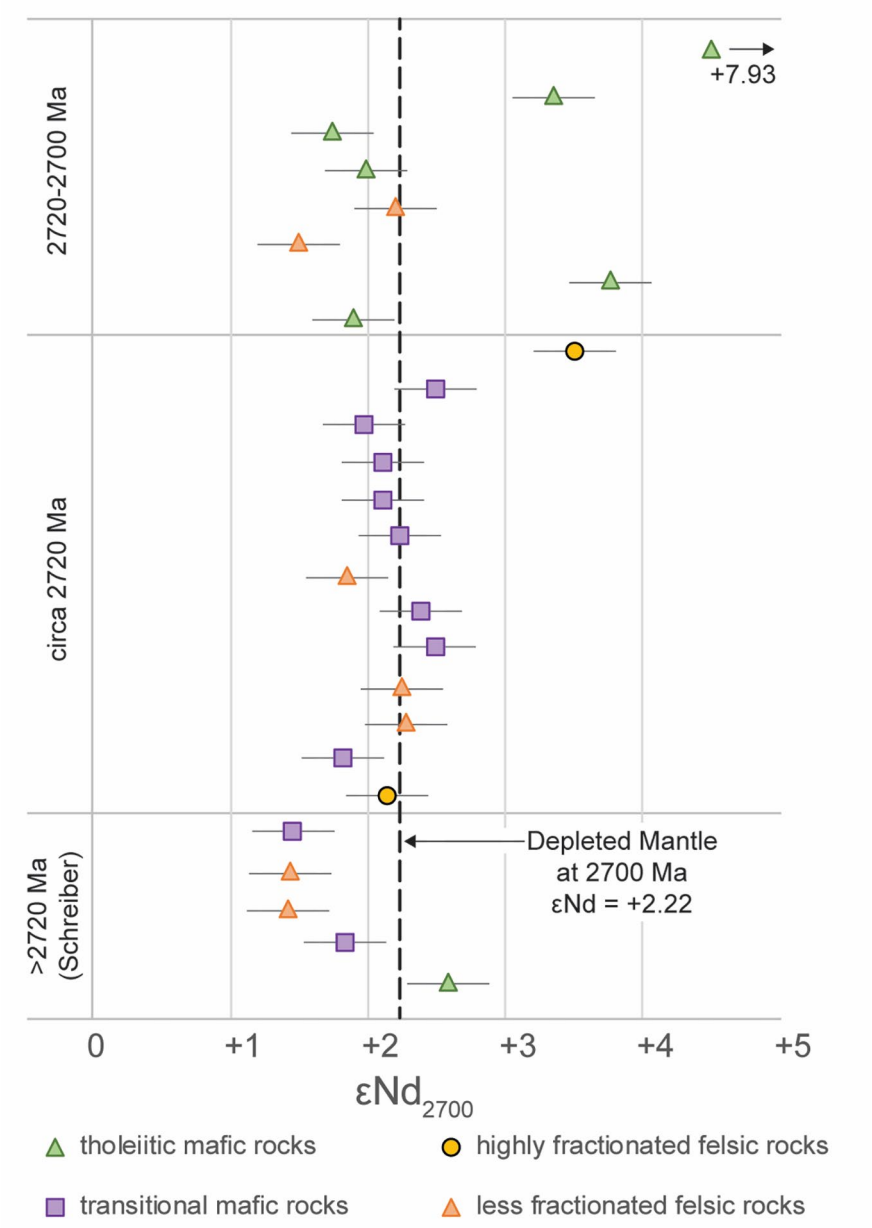

Figure 9. Epsilon Nd (ε_{Nd}) values for all metavolcanic rocks analyzed for Sm-Nd isotope systematics as part of this project. The depleted mantle εNd value at 2700 Ma is included (DePaolo 1981). All ε_{Nd} values are calculated based on an age of 2700 Ma, despite inferred differences in their ages, because precise ages have not been determined for each sample. Estimated error bars of ±0.3 epsilon units have been included to help visualize overlap between samples and deviation outside of error from the Depleted Mantle line. The vertical position of samples within each stratigraphic unit is not representative of the stratigraphic position of each individual sample. Raw data for all these samples, as well as analyzed samples of intrusive rocks, is available in Magnus (2021b).

This stratigraphy records a repeated shift between abundant, geochemically homogenous tholeiitic mafic volcanism, typically associated with extensional tectonic settings, and localized sequences composed of more geochemically diverse, porphyritic mafic and felsic rocks, typically associated with compressional tectonic settings. This repetition indicates a dynamic tectonic setting such as in volcanic arcs associated with convergent plate boundaries. Isotopic data indicate a juvenile volcanic environment typical of an oceanic island arc setting, as opposed to more isotopically mature continental volcanic arc settings.

Significant regional compressional tectonic activity likely initiated after *circa* 2700 Ma as the oceanic arc environment approached and collided with the protocontinental Wabigoon terrane (consistent with interpretations by Williams (1989) and Fralick, Purdon and Davis (2006)). This tectonism sustained upper amphibolite facies pressures and temperatures until *circa* 2680 Ma, after which compressional tectonism relaxed and posttectonic plutons were emplaced.

RECOMMENDATIONS FOR EXPLORATION AND FUTURE WORK

Starved successions I and II correlate with known gold and base metal occurrences. Because these horizons are relatively thin, they are not always easy to locate in the field. However, because they mark the boundaries between tholeiitic and transitional mafic volcanism, detailed mapping and geochemical sampling programs in the Big Duck Lake and Owl Lake area, Goodchild Lake area, and potentially in the nearby Manitouwadge and Shebandowan greenstone belts, may help trace the location of these horizons and could potentially be used as a mineral exploration tool.

In terms of the felsic metavolcanic rocks, the highly fractionated rocks are geochemically similar to those for FII to FIII dacites and rhyolites, and the ambiguous felsic rocks are more similar to FI dacites and rhyolites (Lesher et al. 1986). Hart, Gibson and Lesher (2004) interpret an extensional and/or rifting magmatic environment for generating the FII to FIII rocks, which conflicts with the observation herein that these rocks require greater residence time in the crust (likely in magma chambers, based on petrographic and geochemical evidence for significant fractional crystallization, both in the felsic rocks and their associated porphyritic, transitional mafic volcanic rocks). A more in-depth study into the petrography and geochemistry of the highly fractionated rocks in the Schreiber–Terrace Bay greenstone belt is required to better understand the genesis of these rhyolites and their tectonic significance. If it can be shown that one or more of the local quartz porphyritic intrusions or dikes contributed to this volcanism, then they would be suitable candidates for studying the significance of this highly fractionated signature. Several opportunities for this type of study are present in the greenstone belt, as follows:

- The quartz and feldspar porphyritic North Shore intrusion south of Schreiber, has a synvolcanic age of 2722.6±1.1 Ma (*see* Figure 2, geochronology location 9; Table 1), however, the single geochemical sample from this intrusion does not display highly fractionated trace element characteristics.
- Some quartz and feldspar porphyritic felsic samples of the Lunch Lake pluton (*see* Figure 2, geochronology location 21) display highly fractionated trace element characteristics, and more mafic phases of the intrusion have transitional chemistry; however, the age of this intrusion is yet to be determined.
- The enigmatic felsic intrusive and volcanic rocks of *circa* 2710 Ma age identified in the northern part of the study area (*see* Figure 2, geochronology points 16 and 17) do display this highly fractionated signature. A more detailed mapping and geochemical sampling program focussing on the intrusive and volcanic rocks in this area is required to better understand the significance of these rocks within the greenstone belt and may provide an ideal location to study the petrogenesis of the highly fractionated felsic rocks.

Because FII to FIII felsic volcanic rocks are more likely to be associated with volcanogenic massive sulphide mineralization (Lesher et al. 1986; Hart, Gibson and Lesher 2004), a more in-depth study into the felsic metavolcanic rocks in this greenstone belt could be valuable to the mineral exploration community, and the potential for studying equivalent intrusive and extrusive rocks preserved in this highly accessible greenstone belt could help to better understand the petrogenesis of these felsic rocks and the nature of their relationship with gold and base metal mineralization.

Part 2. Mesoproterozoic Geology of the North Shore of Lake Superior, Terrace Bay Area

INTRODUCTION

The Keweenawan Midcontinent Rift event at *circa* 1100 Ma emplaced a multitude of intrusive and volcanic igneous rocks around present-day Lake Superior. Previous work on these rocks along the north shore of Lake Superior has mainly focused on the Thunder Bay, Lake Nipigon and Marathon areas. The Terrace Bay area (Figure 10), which was a significant gap in our knowledge and understanding of the Midcontinent Rift, was the subject of a regional bedrock mapping project during the field seasons of 2015, 2016, 2017 and 2018 (Magnus and Walker 2015, Magnus and Arnold 2016, Magnus 2017b and Magnus and Hastie 2018). As a result of this project, 3 sets of diabase dikes and 1 set of stock-like intrusions are described and correlated with several previously described suites of magmatic rocks related to the Keweenawan Midcontinent Rift event.

Four 1:20 000 scale bedrock geology maps generated as part of this project cover the Schreiber–Terrace Bay area (Magnus 2017a, Magnus 2019a, Magnus 2021a and Hastie and Magnus 2021a). These maps are accompanied by 4 Miscellaneous Release—Data reports that contain field observations, typical rock type photographs and geochemical data (among other data) (Magnus 2018, 2019b and 2021b; Hastie and Magnus 2021b).

REGIONAL GEOLOGY

The Keweenawan Midcontinent Rift event was a protracted magmatic event spanning 20 to 30 million years that emplaced a multitude of intrusive and volcanic igneous rocks into and on top of the former continent Laurentia, in the vicinity of present-day Lake Superior.

The igneous rocks related to the Midcontinent Rift are incredibly diverse for several reasons:

- The longevity of the rifting event favours diverse magmatic products, as the conditions of melting in the mantle and lower crust typically change through time during short-lived magmatic events.
- The vast area affected by the rifting event favours diverse magmatic products, as the mantle and lower crustal melt sources are likely to have different compositions in different areas. Additionally, through time, the composition of these melt sources can change as progressive melts are removed.
- The heterogeneous geochemical and rheological properties of the Laurentian crust in the Lake Superior region favour diverse magmatic products. Separate magmas rising through only Archean crust (predominantly crystalline intrusive and metamorphic rocks) or through both Archean and overlying Paleoproterozoic crust (varied clastic and chemical sedimentary rocks) would acquire geochemical characteristics according to the unique sequence of crustal materials that could be assimilated that they encounter.

Because of these properties inherent to the Midcontinent Rift environment, the igneous rocks emplaced at different locations and at different times in the Midcontinent Rift tend to have distinct, identifiable geochemical characteristics that allow for geochemical correlation between units. Ongoing research by several authors *(see* references in Cundari et al. 2021) has been aimed at characterizing and cataloguing the separate magmatic suites of the Midcontinent Rift, comparing their geochemistry and morphology to interpret the geodynamic setting of the rift event, and utilizing geochronology to construct a geological history of the rift event (all most recently summarized in Bleeker et al. 2020).

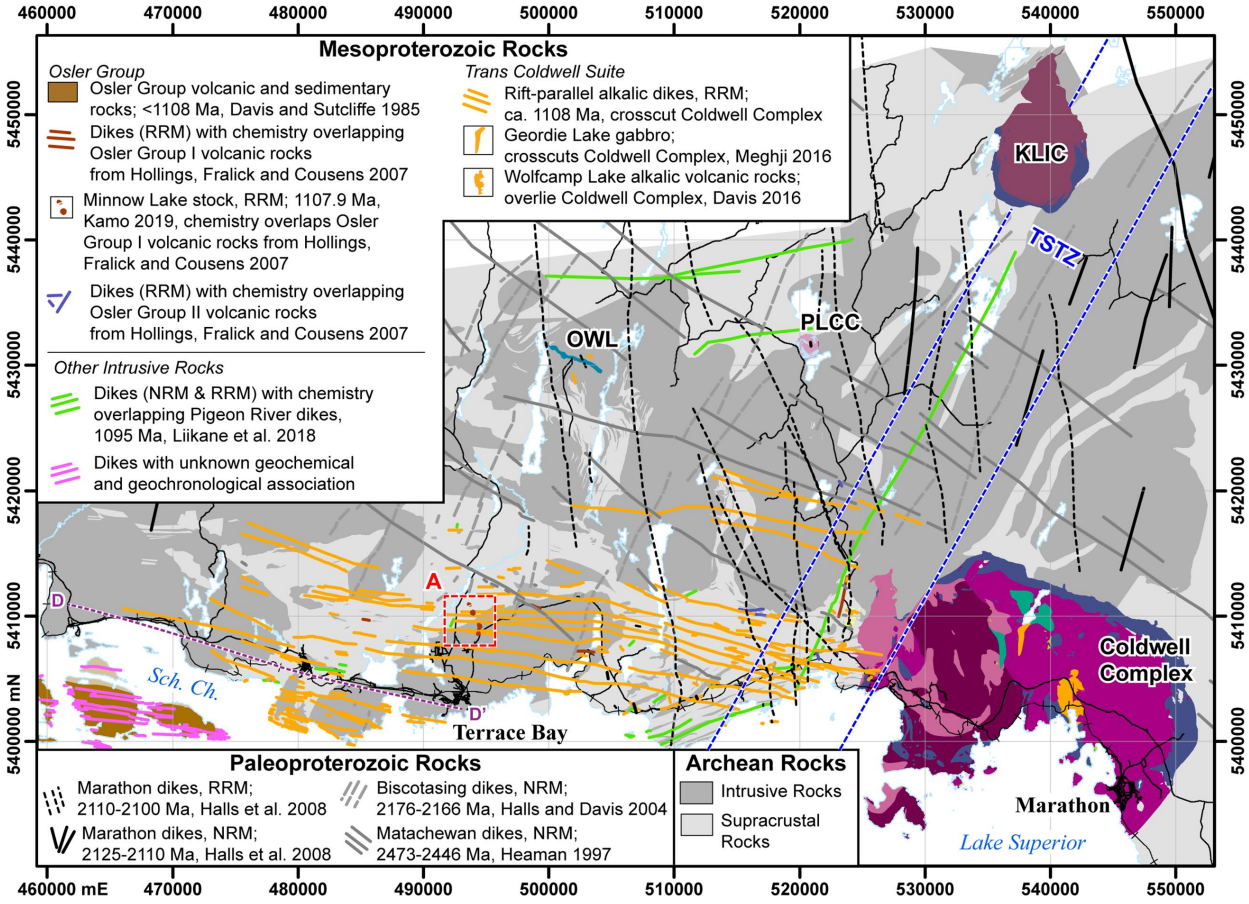

Figure 10. Simplified geological map of the Terrace Bay area along the north shore of Lake Superior, highlighting the Mesoproterozoic geology related to the *circa* 1108 Ma Keweenawan Midcontinent Rift event. The line D–D' separates 2 groups of alkalic diabase dikes: those with reverse remanent magnetization (RRM) to the north and those with normal remanent magnetization (NRM) to the south. The red box labelled "A" outlines the field of view in Figure 13. Abbreviations: KLIC, Killala Lake intrusive complex; OWL, Owl Lake intrusion; PLCC, Prairie Lake carbonatite-ijolite intrusive complex; Sch. Ch., Schreiber Channel; TSTZ, Trans–Superior Tectonic Zone.

GEOCHEMICAL CORRELATION

Several groups of Mesoproterozoic dikes and other intrusive rocks in the Terrace Bay area are correlated with known Midcontinent Rift-related igneous suites; their geochemical characteristics and the factors used in correlation are described herein. A summary of the 100 samples used in this analysis that correlate with known igneous suites is presented in Table 2. Full geochemical data for these samples can be found in Magnus (2018, 2019b, 2021b) and Hastie and Magnus (2021b).

Alkalic Diabase Dikes

The most prominent Mesoproterozoic feature in the Terrace Bay area west of the Coldwell alkalic intrusive complex are the west-northwest–trending dikes that crop out along the Lake Superior shoreline and occur up to 20 km inland (*see* Figure 10). North of the town of Terrace Bay, these dikes correlate with negative aeromagnetic anomalies on regional aeromagnetic maps; south of the town of Terrace Bay, they correlate with positive aeromagnetic anomalies (*see* Figure 10, line D–D'; Ontario Geological Survey 2003).

These dikes are composed of ophitic to subophitic-textured olivine gabbro with generally fayalitic (iron-rich) olivine (average composition Fo_{30}), clinopyroxene (dominantly magnesium-rich augite), intermediate plagioclase (andesine to bytownite) and minor alkali feldspar. On a weathered surface, iron-rich inclusions in feldspars and pyroxenes are oxidized and impart a reddish-brown hue to these rocks, which can help to distinguish them from other diabase dikes, typically black to greenish black, in the Terrace Bay area. Fayalitic (iron-rich) olivine is typically associated with alkalic igneous rocks, whereas olivine in subalkalic rocks tends to be more magnesium-rich (forsterite).

Based on major element contents, these rocks are alkalic (Irvine and Baragar 1971) and classify as basalts, trachy-basalts and tephrite-basanite on a Total Alkalis versus Silica (TAS) diagram (Le Maitre 1989). The "alkalic" classification is used herein as a descriptive name for this group of diabase dikes.

Trace element concentrations in these rocks are elevated, around 100 times greater than Primitive Mantle (PM) values for the lithophile elements and light rare earth elements, dropping steeply to 10 times PM values for the incompatible elements (Figure 11A). There is no enrichment of Th over Nb and Ta in these rocks. The patterns display consistent negative anomalies in K, Rb, Sr and Pb, all fluid-mobile elements, and negative anomalies in P, Zr, Ti and Sc.

The trace element characteristics for these rocks are similar to those for the Wolfcamp Lake alkalic basalts that overlie the Coldwell alkalic intrusive complex to the east (*see* Figures 11A and 10; Davis 2016; Davis, Hollings and Cundari 2017). These trace element characteristics are also similar to portions of the Geordie Lake gabbro, which intrudes the Coldwell alkalic intrusive complex (Meghji 2016) and several northwest-striking dikes in the nearby Pukaskwa area, south of the Coldwell alkalic intrusive complex (Cundari et al. 2021).

A subset of these alkalic dikes was observed in the Terrace Bay area, generally located close to the Coldwell alkalic intrusive complex. These dikes have a trachytic texture with abundant elongate plagioclase crystals. Iron inclusions in these feldspars are typically oxidized in these rocks, which imparts a distinct, bright reddish-orange-brown hue to the rocks in outcrop. These rocks plot as trachy-andesites on the TAS diagram (Le Maitre 1989), and their trace element patterns are more enriched than their mafic counterparts, with greatly exaggerated negative anomalies in P and Ti, consistent with fractionation of accessory minerals like apatite and titanite (Figure 11B). Compared to their mafic counterparts, the trachytic-textured rocks display depletion in Cs and Ba, a more pronounced depletion in Sr and an

Table 2. List of samples of diabase dikes in the Terrace Bay area for which there is whole rock major and trace element geochemistry, available in the associated Miscellaneous Release—Data, listed under the MRD column (*see* Magnus 2018, 2019b, 2021b, Hastie and Magnus 2021b). Each sample in this table has been assigned to one of the magmatic suites discussed in this report; these labels are either not included or up to date in the MRDs. There are only a handful of samples included in the MRDs that have not been assigned to one of these suites. Abbreviations: MRD = Miscellaneous Release—Data.

Sample	Intrusive Suite	MRD	Sample	Intrusive Suite	MRD
18EGH012A	Minnow Lake stock	382	15SJM074A	alkalic diabase	361
18EGH013-2	Minnow Lake stock	382	15SJM111E	Trans–Coldwell Suite	361
18EGH013A	Minnow Lake stock	382	15SJM112E	Trans–Coldwell Suite	361
18EGH014A	Minnow Lake stock	382	15SJM118B	Trans–Coldwell Suite	361
18EGH015-2	Minnow Lake stock	382	15SJM128B	Trans–Coldwell Suite	361
15SJM004A	Lower Osler Group dike	361	15SJM157C	Trans–Coldwell Suite	361
15SJM115C	Lower Osler Group dike	361	15SJM171B	Trans–Coldwell Suite	361
16SJM166A	Lower Osler Group dike	361	15SJM210C	Trans–Coldwell Suite	361
17KAM057B	Lower Osler Group dike	375	16KA002B	Trans–Coldwell Suite	361
17SJM048D	Lower Osler Group dike	375	16KA099A	Trans–Coldwell Suite	361
18EM014B	Lower Osler Group dike	382	16KAM013B	Trans–Coldwell Suite	382
18EM072A	Lower Osler Group dike	382	16SJM001B	Trans–Coldwell Suite	361
18SJM027A	Lower Osler Group dike	381	16SJM004B	Trans–Coldwell Suite	361
15JW047F	Upper Osler Group dike	361	16SJM004C	Trans–Coldwell Suite	361
15JW107I	Upper Osler Group dike	382	16SJM007B	Trans–Coldwell Suite	361
15SJM022D	Upper Osler Group dike	361	16SJM008A	Trans–Coldwell Suite	361
15SJM145C	Upper Osler Group dike	361	16SJM009B	Trans–Coldwell Suite	361
16KA080F	Upper Osler Group dike	361	16SJM010A	Trans–Coldwell Suite	361
16SJM021A	Upper Osler Group dike	361	16SJM013B	Trans–Coldwell Suite	361
16SJM054A	Upper Osler Group dike	361	16SJM029B	Trans–Coldwell Suite	375
17KAM061B	Upper Osler Group dike	375	16SJM042B	Trans–Coldwell Suite	361
18EM119A	Upper Osler Group dike	381	16SJM050B	Trans–Coldwell Suite	361
18SJM103B	Upper Osler Group dike	381	16SJM060B	Trans–Coldwell Suite	361
15JW054B	Pigeon River dike	361	16SJM076A	Trans–Coldwell Suite	361
15JW071B	Pigeon River dike	361	16SJM142B	Trans–Coldwell Suite	361
15SJM068B	Pigeon River dike	375	16SJM144B	Trans–Coldwell Suite	361
15SJM170B	Pigeon River dike	361	16SJM145B	Trans–Coldwell Suite	361
15SJM188B	Pigeon River dike	361	16SJM147B	Trans–Coldwell Suite	381
16SJM026C	Pigeon River dike	375	16SJM148B-1	Trans–Coldwell Suite	381
16SJM127A	Pigeon River dike	361	16SJM148B-2	Trans–Coldwell Suite	381
16SJM139A	Pigeon River dike	375	16SJM151A	Trans–Coldwell Suite	375
16SJM144A	Pigeon River dike	361	16SJM175B	Trans–Coldwell Suite	361
16SJM146E	Pigeon River dike	361	16SJM178D	Trans–Coldwell Suite	361
16SJM162A	Pigeon River dike	361	16SJM180B	Trans–Coldwell Suite	361
18EM065B	Pigeon River dike	382	16SJM181A	Trans–Coldwell Suite	361
18EM066C	Pigeon River dike	381	16SJM181B	Trans–Coldwell Suite	361
18SJM049A	Pigeon River dike	381	16SJM200A	Trans–Coldwell Suite	361
15JW004B	Trans–Coldwell Suite	361	16WM023-2	Trans–Coldwell Suite	361
15JW008A	Trans–Coldwell Suite	361	16WM045A	Trans–Coldwell Suite	361

Sample	Intrusive Suite	MRD	Sample	Intrusive Suite	MRD
15JW030C	Trans–Coldwell Suite	361	17KAM067B	Trans–Coldwell Suite	382
15JW047C	Trans–Coldwell Suite	361	18EM003B	Trans–Coldwell Suite	382
15JW054C	Trans–Coldwell Suite	361	18SJM023B	Trans–Coldwell Suite	381
15JW067A	Trans–Coldwell Suite	375	15SJM019B	alkalic diabase - Trachytic	361
15JW072C	Trans–Coldwell Suite	375	15SJM025B	TCS - Trachytic	361
15JW102B	Trans–Coldwell Suite	361	15SJM112D	TCS - Trachytic	361
15SJM022B	Trans–Coldwell Suite	361	15SJM175A	TCS - Trachytic	361
15SJM031	Trans–Coldwell Suite	361	16KA048B	TCS - Trachytic	361
15SJM053C	Trans–Coldwell Suite	361	16SJM001C	TCS - Trachytic	361
15SJM053D	Trans–Coldwell Suite	361	16SJM001E	TCS - Trachytic	361
15SJM067B	Trans–Coldwell Suite	375	16SJM111C	TCS - Trachytic	361

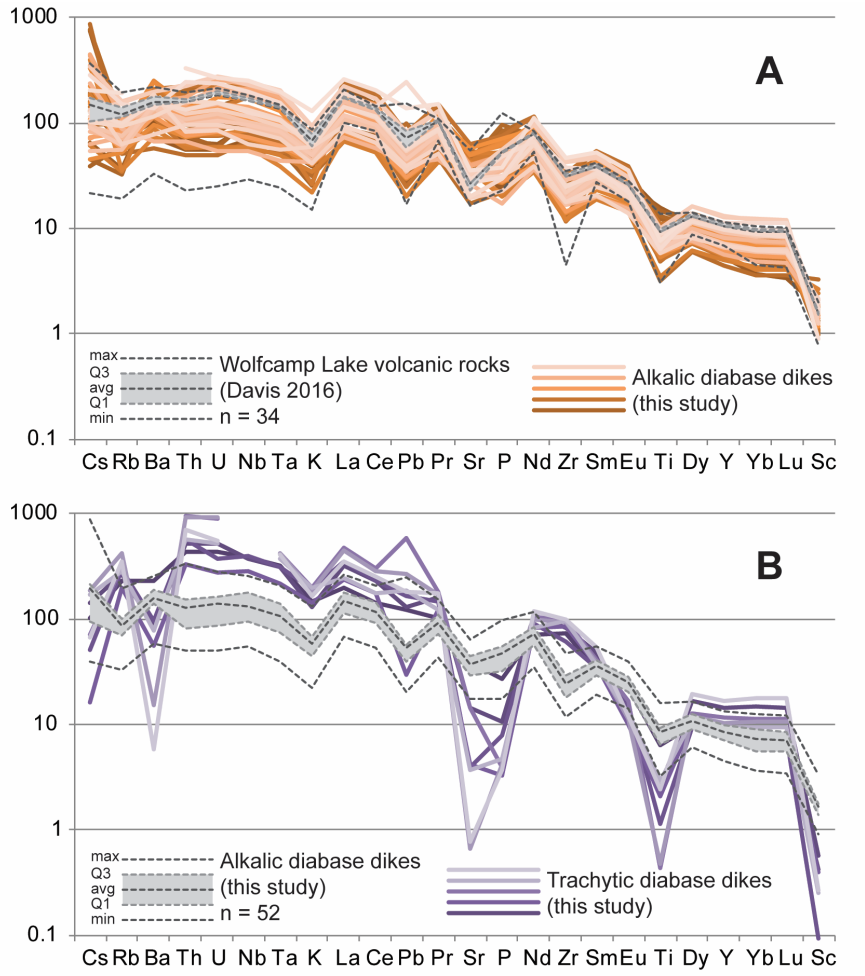

Figure 11. Trace element diagrams normalized to Primitive Mantle values (Sun and McDonough 1995). **A)** Average composition of Wolfcamp Lake volcanic rocks, located in the nearby Coldwell alkalic intrusive complex (Davis 2016), plotted above samples of alkalic diabase dikes in the Terrace Bay area that display similar trace element characteristics. **B)** Average composition of alkalic diabase dikes in the Terrace Bay area (as displayed in A) plotted above samples of trachytic-textured alkalic dikes in the Terrace Bay area. Abbreviations: avg, average; max, maximum value; min, minimum value; Q1, first quartile value; Q3, third quartile value.

enrichment in Rb, which suggests these rocks are related to their mafic counterparts by some complicated fractional crystallization of feldspars, feldspathoids, or a mix of both. The trachytic-textured rocks are also slightly enriched in Pb and Zr compared to their mafic counterparts.

Five samples of alkalic diabase dikes, including one trachytic dike, were submitted for Sm-Nd and Sr-Rb isotopic analysis (Magnus 2021b). Values for $^{143}Nd/^{144}Nd_{1100}$ (0.51109, 0.51120, 0.51121, 0.51124 and 0.51127) are very close to the same value for the chondrite uniform reservoir (CHUR) at 1100 Ma (0.51122, Hamilton et al. 1983). Values for $^{87}Sr/^{86}Sr_{1100}$ (0.6957, 0.6992, 0.7030, 0.7059 and 0.7303) generally deviate above and below the same value for CHUR at 1100 Ma (0.7031, Workman and Hart 2005); this deviation is likely caused by the fluid-mobile nature of these alkali metals, though whether the mobilization was related to late magmatic fluids or subsequent hydrothermal alteration is unknown. The near chondritic $^{143}Nd/^{144}Nd_{1100}$ values are consistent with the same values for nearby mafic alkalic rocks (Good et al. 2021).

The alkalic diabase has been observed crosscutting and being crosscut by syenitic rocks at the western edge of the Coldwell alkalic intrusive complex (*circa* 1108 Ma), which constrains these dikes to approximately the same age. Based on their similar major and trace element and isotopic geochemistry and their close proximity to the Wolfcamp Lake volcanic rocks, Geordie Lake gabbro and the dikes in Pukaskwa area, these alkalic diabase dikes are considered part of the same magmatic event as these other mafic alkalic rocks. Good et al. (2021) considers the relationship between all of the nearby mafic alkalic rocks and includes a more in-depth analysis of their major and trace element and isotopic systematics.

Pigeon River Dikes

A set of east-northeast–trending dikes crop out along the Lake Superior shoreline between Terrace Bay and the Coldwell alkalic intrusive complex and occur sporadically elsewhere in the Terrace Bay area (*see* Figure 10). These dikes correlate with positive aeromagnetic anomalies (Ontario Geological Survey 2003).

These east-northeast–trending dikes are composed of ophitic- to subophitic-textured gabbro with basaltic major element concentrations (Le Maitre 1989).

On a primitive-mantle–normalized trace element diagram, the patterns for these rocks display a low negative slope and are enriched in fluid mobile, lithophile elements, including Cs, Rb, Ba, Pb and Th (Figure 12A). These trace element characteristics are the same as those for the Pigeon River dikes located south of the city of Thunder Bay and on the Sibley Peninsula, which are along-strike with the dikes in the Terrace Bay area, but separated by approximately 200 km across northern Lake Superior (Cundari et al. 2021).

Based on the similar trace element characteristics and their location along-strike from the established Pigeon River dike swarm, these east-northeast–trending dikes are considered an eastward extension of that dike swarm, which were emplaced at *circa* 1095 Ma (Liikane et al. 2018).

Osler Group Rocks—Minnow Lake Stock

A small circular, stock-like intrusion, approximately 100 m in diameter, was observed in outcrop on Minnow Lake, east of the Longlac Backroad north of the town of Terrace Bay (*see* Figure 10; Figure 13A). This intrusion correlates with a distinct, circular, negative aeromagnetic anomaly (Figure 13B). Three other potential small intrusions have been tentatively outlined south of the Minnow Lake stock based on similar aeromagnetic anomalies observed in the first and second vertical derivative aeromagnetic images (*see* Figure 13).

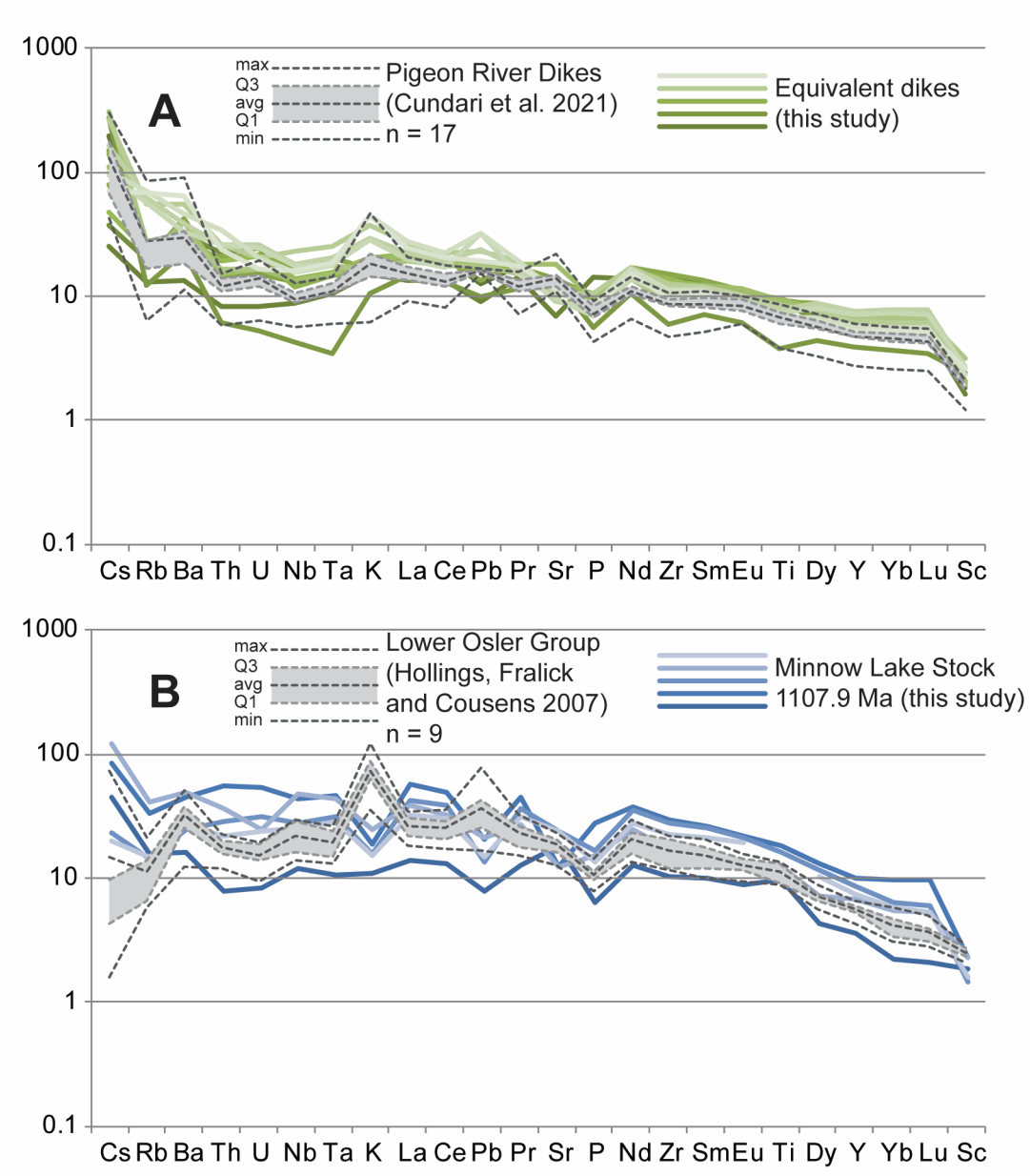

Figure 12. Trace element diagrams normalized to Primitive Mantle values (Sun and McDonough 1995). **A)** Average composition of Pigeon River dikes (Cundari et al. 2021) plotted above samples of diabase dikes in the Terrace Bay area that display similar trace element characteristics. **B)** Average composition of volcanic rocks in the lower part of the Osler Group (Hollings, Fralick and Cousens 2007) plotted above samples from the Minnow Lake stock, which display similar trace element characteristics. Abbreviations: avg, average; max, maximum value; min, minimum value; Q1, first quartile value; Q3, third quartile value.

The Minnow Lake stock is composed of medium- to coarse-grained ophitic-textured gabbro with basaltic major element concentrations (Le Maitre 1989).

On a PM-normalized trace element diagram, the patterns for the Minnow Lake intrusive rocks display a moderate negative slope with a distinct enrichment in Cs and depletion in K, Pb (Figure 12B). These trace element patterns are similar to those of the volcanic rocks in the lower part of the Osler Group (Hollings, Fralick and Cousens 2007), located southwest of the Terrace Bay area (*see* Figure 10). Despite the similar overall trend of all of these rocks, the volcanic rocks are depleted in Cs enriched in K and Pb, mirroring the enrichment and depletion of those elements in the intrusive rocks in the Minnow Lake stock. This indicates that in this magmatic system, Cs is being sequestered in the lower parts of the system, whereas K and Pb remain in the melt and are concentrated in the latest phases to crystallize.

Two samples of the Minnow Lake stock were submitted for Sm-Nd and Sr-Rb isotopic analysis (Magnus 2021b). Values for $^{143}Nd/^{144}Nd_{1100}$ (0.51131 and 0.51129) are slightly more depleted than CHUR at 1100 Ma (0.51122, Hamilton et al. 1983), and $^{87}Sr/^{86}Sr_{1100}$ values (0.70271 and 0.70297) are close to the same value for the CHUR at 1100 Ma (0.7031, Workman and Hart 2005). These values are slightly more depleted than the near-chondritic values for the lower Osler Group volcanic rocks (Hollings, Fralick and Cousens 2007); however, more depleted (less contaminated) values are expected for these intrusive rocks because during emplacement they were not exposed to the isotopically mature Paleoproterozoic sedimentary rocks that the Osler Group volcanic rocks were erupted through.

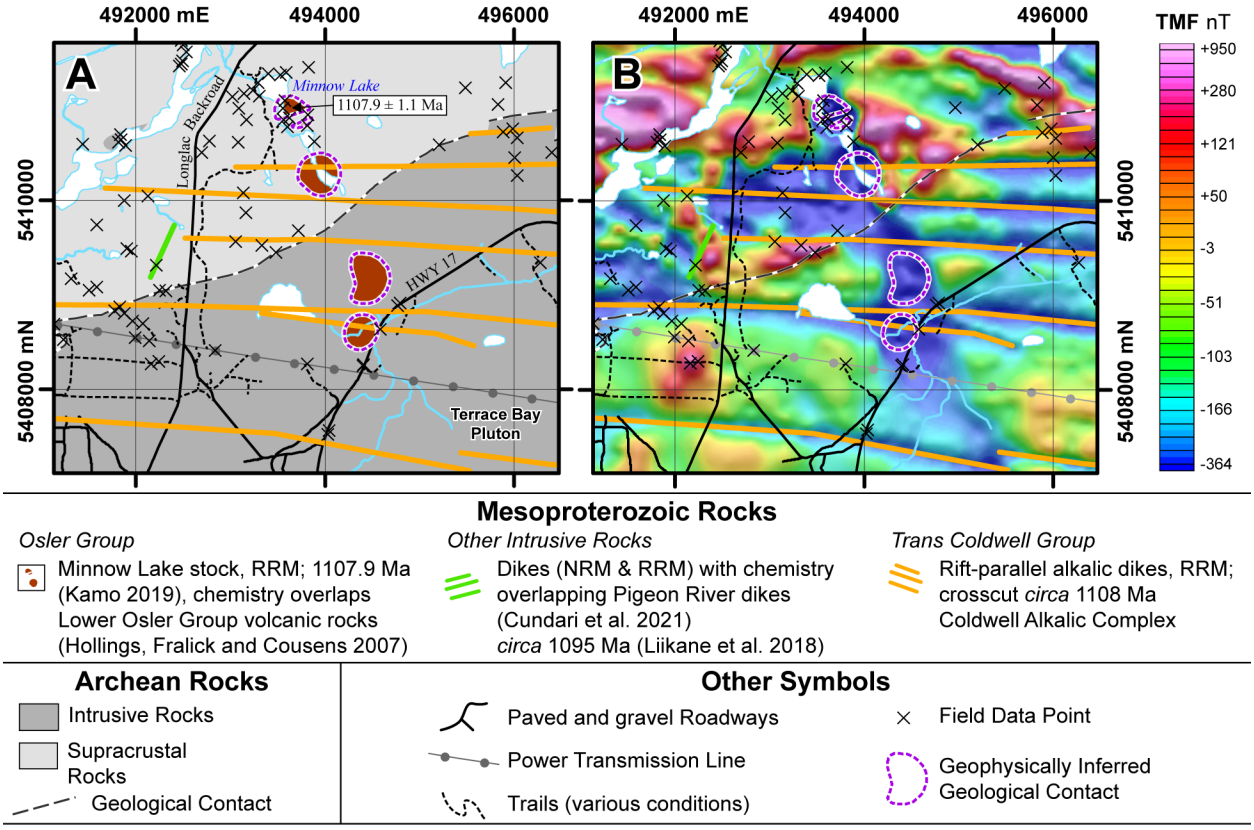

Figure 13. A) Simplified bedrock geology map outlining an area north of the town of Terrace Bay (*after* Hastie and Magnus 2021a; *see* Figure 10, red box labelled A). **B)** Map of the total magnetic field covering the same area as in A (Ontario Geological Survey 2003). Abbreviations: Ma, million years; NRM, normal remanent magnetisation; RRM, reverse remanent magnetisation; nT, nanoteslas (units); TMF, total magnetic field.

One sample of the Minnow Lake stock was submitted for geochronological analysis. U/Pb analysis of baddeleyite by thermal-ionization mass spectrometry resulted in an age of 1107.9 ± 1.1 Ma (Kamo 2019a). This is roughly correlative with the interpreted age for the lower part of the Osler Group volcanic rocks, consistent with their correlation using geochemistry (Hollings, Fralick and Cousens 2007).

Osler Group Rocks—Dikes

A small population of dikes located throughout the Terrace Bay area are distinguished solely based on their geochemical characteristics. These dikes are generally parallel to the west-northwest–trending alkalic diabase dikes, and thus appear to have ascended using the same magmatic plumbing system.

These dikes are composed of ophitic- to subophitic-textured gabbro with basaltic major element concentrations (Le Maitre 1989).

These dikes are split into 2 groups based on their trace element characteristics (Figure 14). On PM-normalized trace element diagrams, both groups display moderate negative slopes in their rare earth element contents (La to Lu); however, the 2 groups are distinguished particularly by the enrichment and depletion of the lithophile elements Th and U in each group (*see* Figure 14). These 2 groups correlate well with the trace element characteristics of the lower and upper groups of the Osler Group volcanic rocks. Similar to the correlation described for the Minnow Lake stock, these intrusive rocks are enriched in Cs and depleted in the fluid mobile elements K and Pb compared to their volcanic counterparts. This supports the interpretation that in this magmatic system, Cs is being sequestered in the lower part of the system (likely by fractional crystallization of some cesium-rich mineral), and K and Pb remain in the melt (likely in volcanic fluids) and are concentrated in the magma until the latest stages of eruption.

Based on their similar trace element characteristics and their close proximity to the preserved Osler Group volcanic rocks, these dikes are considered to represent intrusive parts of the magmatic system that fed the overlying Osler Group volcanic rocks.

Trans–Superior Tectonic Zone—An Observation

The general trend of the dikes within each of the groups described herein are consistent throughout most of the Terrace Bay area. The exception to this observation is within the boundaries of the Trans–Superior Tectonic Zone (TSTZ), an interpreted northeast-trending crustal-scale structure that is generally believed to represent the initial stage of the failed “third arm” of the Midcontinent Rift system (*see* Figure 10). In the vicinity of the TSTZ, rocks belonging to the alkalic dikes (*circa* 1108 Ma), the Osler Group dikes (*circa* 1108 Ma) and the Pigeon River dikes (*circa* 1095 Ma) were observed in outcrop with deviant trends that strike parallel to the TSTZ. These changes in trends support the hypothesis that the TSTZ represented a significant crustal-scale feature throughout the Midcontinent Rift event, and if rifting along the TSTZ had continued, the TSTZ might have been a significant conduit for local magmatism.

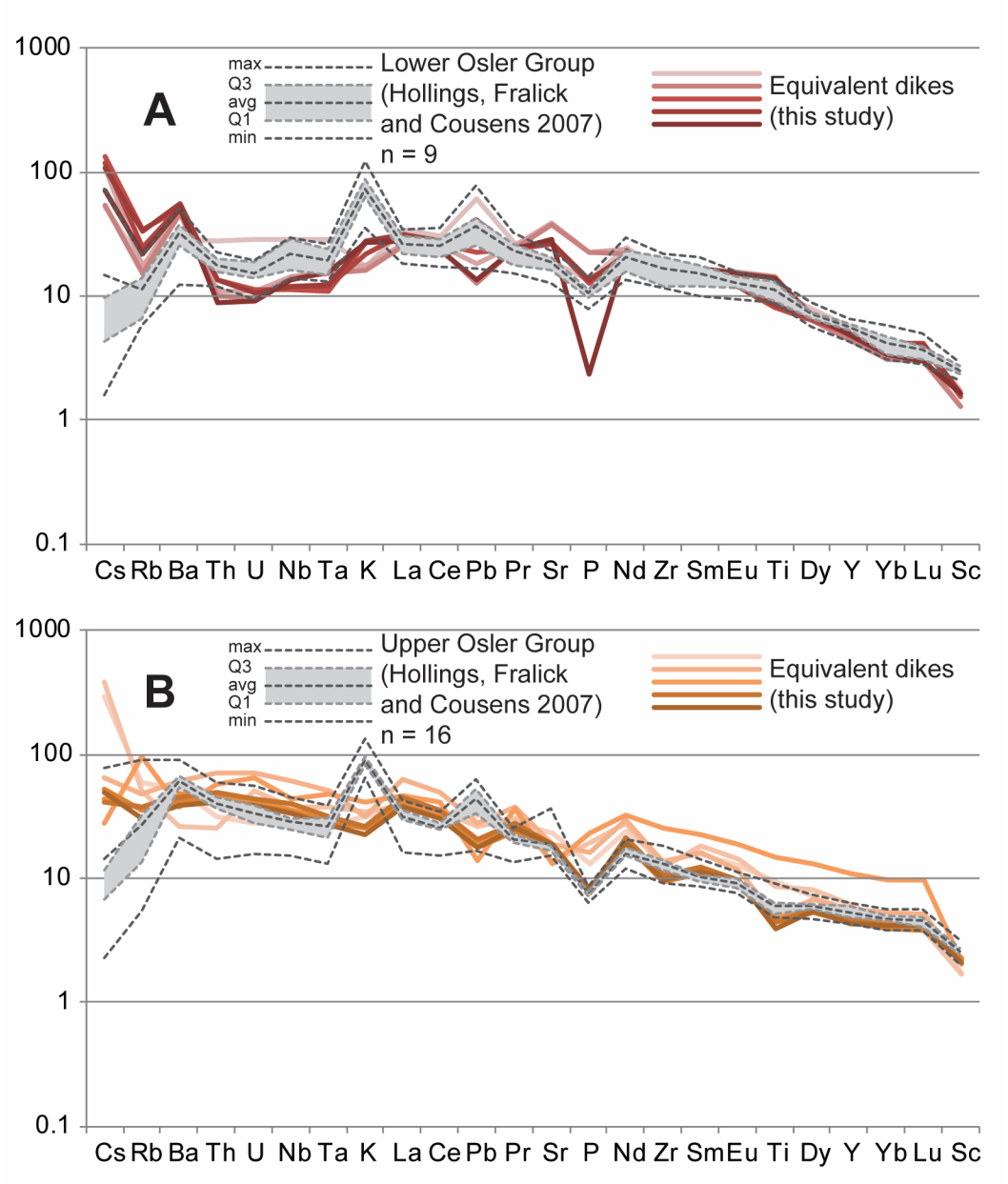

Figure 14. Trace element diagrams normalized to Primitive Mantle values (Sun and McDonough 1995). **A)** Average composition of volcanic rocks in the lower part of the Osler Group volcanic rocks (Hollings, Fralick and Cousens 2007) plotted above samples of diabase dikes in the Terrace Bay area that display similar trace element characteristics. **B)** Average composition of volcanic rocks in the upper part of the Osler Group volcanic rocks (Hollings, Fralick and Cousens 2007) plotted above samples of diabase dikes from the Terrace Bay area that display similar trace element characteristics. Abbreviations: avg, average; max, maximum value; min, minimum value; Q1, first quartile value; Q3, third quartile value.

SUMMARY

This detailed mapping and sampling program has allowed for several important correlations within the Midcontinent Rift environment along the north shore of Lake Superior.

- Abundant alkalic diabase dikes in the Terrace Bay area correlate with several other alkalic mafic intrusive and volcanic rocks in the north shore area. This suite of alkalic mafic rocks represents a significant magmatic event within the local Midcontinent Rift environment which until recently was not recognized.
- A subset of diabase dikes in the Terrace Bay area correlate with the Pigeon River dike swarm in the Thunder Bay area, roughly 200 km to the west along-strike. This greatly expands the footprint of this dike swarm.
- A subset of diabase dikes and several stock-like intrusions in the Terrace Bay area correlate with the upper and lower Osler Group volcanic rocks, located just to the southwest of the Terrace Bay area. The positive identification of intrusive rocks related to the volcanic rocks provides a unique opportunity to study the nature of near-surface magmatism in the Midcontinent Rift environment.

RECOMMENDATIONS FOR FUTURE WORK

Following completion of this mapping and sampling program, there remains one large knowledge gap for Midcontinent Rift-related diabase dikes along the north shore of Lake Superior: the shoreline west of the Schreiber Channel (*see* Figure 10) to the Sibley Peninsula, which was the subject of a sampling program by Carl (2011)(geochemistry included in Cundari et al. 2021). This data gap includes the Black Bay Peninsula, Simpson Island, Copper Island and other islands in that archipelago. This area was the subject of a mapping and sampling program that focussed on the volcanic rocks (Hollings, Fralick and Cousens 2007); however, this shoreline exposes abundant diabase dikes of unknown geochemical composition.

Additionally, the confirmed presence of intrusive rocks related to the Osler Group volcanic rocks provides a unique opportunity to study the processes that generated the Osler Group volcanic rocks, which may help elucidate the nature of magmatism within the Midcontinent Rift environment in general. The author recommends a more in-depth investigation of the relationship between these intrusive and volcanic rocks.

Acknowledgments

Part 1 of this report benefited from insightful discussions with a great number of colleagues, including Dr. E. Hastie, who co-supervised the 2018 field season, Dr. R.M. Easton, L. Ratcliffe, R. Metsaranta, and T. Gemmell. Part 2 of this report benefited from discussions with Dr. R.M. Easton, Dr. P. Hollings, Dr. D. Good, R. Metsaranta, R. Cundari and J. McBride. The author would also like to thank members of his Ontario Geological Survey field crews during the 2015, 2016, 2017 and 2018 field seasons, without whom the collection of the vast database used in Part 1, and the collection of all the diabase samples used in Part 2, would not have been possible. Thanks also to M. Smyk, D. Campbell and M. Puumala of the Resident Geologist Program, Thunder Bay office, for their help during this project. Finally, thanks to the people of Pic River and Pic Mobert First Nations communities for their gracious blessing and for allowing us to work on their traditional lands.

References

Addison, W.D., Brumpton, G.R., Vallini, D.A., McNaughton, N.J., Davis, D.W., Kissin, S.A., Fralick, P.W. and Hammond, A.L. 2005. Discovery of distal ejecta from the 1850 Ma Sudbury impact event; Geology, v.33, p.193-196.

Arnold, K.A., Hollings, P. and Magnus, S.J. 2017. Geology and mineral potential of the Terrace Bay pluton, western Schreiber–Hemlo greenstone belt; *in* Summary of Field Work and Other Activities, 2017, Ontario Geological Survey, Open File Report 6333, p.12-1 to 12-6.

——— 2020. Geological and geochemical data from the Terrace Bay pluton, western Schreiber–Hemlo greenstone belt, Wawa–Abitibi terrane, Superior Province, northwestern Ontario; Ontario Geological Survey, Miscellaneous Release—Data 379.

Averalo, R. Jr. and McDonough, W.F. 2010. Chemical variations and regional diversity observed in MORB; Chemical Geology, v.271, p.70-85.

Bleeker, W., Liikane, D.A., Smith, J., Hamilton, M., Kamo, S.L., Cundari, R., Easton, M. and Hollings, P. 2018. Controls on the localization and timing of mineralized intrusions in intra-continental rift systems, with a specific focus on the ca. 1.1 Ga Mid-continent Rift system; *in* Targeted Geoscience Initiative: 2017 report of activities, v.2, Geological Survey of Canada, Open File 8373, p.15-27. https://doi.org/10.4095/306594

Bleeker, W., Smith, J., Hamilton, M., Kamo, S., Liikane, D., Hollings, P., Cundari, R., Easton, M. and Davis, D. 2020. The Midcontinent Rift and its mineral systems: Overview and temporal constraints of Ni-Cu-PGE mineralized intrusions; *in* Targeted Geoscience Initiative 5: Advances in the understanding of Canadian Ni-Cu-PGE and Cr ore systems, Geological Survey of Canada, Open File 8722, p.7-35. https://doi.org/10.4095/326880

Buchan, K.L., Mortensen, J.K. and Card, K.D. 1993. Northeast-trending Early Proterozoic dykes of southern Superior Province: Multiple episodes of emplacement recognized from integrated paleomagnetism and U-Pb geochronology; Canadian Journal of Earth Sciences, v.30, p.1286-1296.

Cannon, W.F., Schulz, K.J., Horton, J.W. and Kring, D.A. 2010. The Sudbury impact layer in the Paleoproterozoic iron ranges of northern Michigan, USA; Geological Society of America Bulletin, v.122, p.50-75.

Carl, C.F. 2011. Geochemistry and petrology of intrusive rocks of the Sibley Peninsula; unpublished BSc thesis, Lakehead University, Thunder Bay, Ontario, Canada, 83p.

Corfu, F. and Stott, G.M. 1998. Shebandowan greenstone belt, western Superior Province: U-Pb ages, tectonic implications, and correlations; Geological Society of America Bulletin, v.110, p.1467-1484.

Cundari, R.M., Puumala, M.A., Smyk, M.C. and Hollings, P. 2021. New and compiled whole-rock geochemical and isotope data of Midcontinent Rift–related rocks, Thunder Bay area; Ontario Geological Survey, Miscellaneous Release—Data 308 – Revised.

Davis, D.W., Ménard, J. and Sutcliffe, C.N. 2018. U-Pb geochronology by LA-ICP-MS in samples from northern Ontario; internal report prepared for the Ontario Geological Survey, Jack Satterly Geochronology Laboratory, University of Toronto, Toronto, Ontario, 94p.

Davis, D.W., Schandl, E.S. and Wasteneys, H.A. 1994. U-Pb dating of minerals in alteration halos of Superior Province massive sulphide deposits: Syngenesis versus metamorphism; Contributions to Mineralogy and Petrology, v.115, p.427-437.

Davis, D.W. and Stott, G.M. 2003. Geochronology of two Proterozoic mafic dike swarms in northwestern Ontario; *in* Summary of Field Work and Other Activities, 2003, Ontario Geological Survey, Open File Report 6120, p.12-1 to 12-7.

Davis, D.W. and Sutcliffe, R.H. 1985. U-Pb ages from the Nipigon Plate and northern Lake Superior; Geological Society of America, Bulletin, v.96, p.1572-1579.

Davis, D.W. and Sutcliffe, C.N. 2017. U-Pb geochronology by LA-ICP-MS in samples from northern Ontario; internal report prepared for the Ontario Geological Survey, Jack Satterly Geochronology Laboratory, University of Toronto, Toronto, Ontario, 131p.

Davis, S. 2016. Petrology and geochemistry of the Wolfcamp Lake basalts; unpublished HBSc thesis, Lakehead University, Thunder Bay, Ontario, 68p.

Davis, S., Hollings, P. and Cundari, R.M. 2017. Geochemistry of the Mesoproterozoic Wolfcamp Lake basalts, northwestern Ontario; Ontario Geological Survey, Miscellaneous Release—Data 345.

DePaolo, D.J. 1981. Neodymium isotopes in the Colorado Front Range and crust-mantle evolution in the Proterozoic; Nature, v.291, p.193-196.

Dickin, A.P. 2018. Radiogenic isotope geology, 3rd edition; Cambridge University Press, Cambridge, United Kingdom, 482p.

Fralick, P., Davis, D.W. and Kissin, S.A. 2002. The age of the Gunflint Formation, Ontario, Canada: Single zircon U-Pb age determinations from reworked volcanic ash; Canadian Journal of Earth Sciences, v.39, p.1085-1091.

Fralick, P., Purdon, R.H. and Davis, D.W. 2006. Neo-Archean trans-subprovince sediment transport in southwestern Superior Province: Sedimentological, geochemical and geochronological evidence; Canadian Journal of Earth Sciences, v.43, p.1055-1070.

Good, D., Hollings, P., Dunning, G., Epstein, R., McBride, J., Jedemann, A., Magnus, S., Bohay, T. and Shore, G. 2021. A new model for the Coldwell Complex and associated dykes in the Midcontinent Rift, Canada; Journal of Petrology, v.62, Issue 7, 43p., published online 23 Aril 2021, ega036, https://doi.org/10.1093/petrology/egab036.

Halls, H.C. and Davis, D.W. 2004. Paleomagnetism and U-Pb geochronology of the 2.17 Ga Biscotasing dyke swarm, Ontario, Canada: Evidence for vertical-axis crustal rotation across the Kapuskasing Zone; Canadian Journal of Earth Sciences, v.41, p.255-269.

Halls, H.C., Davis, D.W., Stott, G.M., Ernst, R.E. and Hamilton, M.A. 2008. The Paleoproterozoic Marathon Large Igneous Province: New evidence for a 2.1 Ga long-lived mantle plume event along the southern margin of the North American Superior Province; Precambrian Research, v.162, p.327-353.

Hamilton, P.J., O'Nions, R.K., Bridgwater, D., and Nutman, A. 1983. Sm-Nd studies of Archaean metasediments and metavolcanics from West Greenland and their implications for the Earth's early history; Earth and Planetary Science Letters, v.62, p.263–272.

Hamilton, M.A. and Stott, G.M. 2008. The significance of new U/Pb baddeleyite ages from two Paleoproterozoic diabase dikes in northern Ontario; *in* Summary of Field Work and Other Activities, 2008, Ontario Geological Survey, Open File Report 6226, p.17-1 to 17-10.

Hart, T.R., Gibson, H.L. and Lesher, C.M. 2004. Trace element geochemistry and petrogenesis of felsic volcanic rocks associated with volcanogenic massive Cu-Zn-Pb sulphide deposits; Economic Geology, v.99, p.1003-1013.

Hastie, E.C.G. and Magnus, S.J. 2021a. Precambrian geology of Strey Township, northwestern Ontario; Ontario Geological Survey, Preliminary Map P.3846, scale 1:20 000.

——— 2021b. Geological, geochemical and petrographic data from Strey Township, western Schreiber–Hemlo greenstone belt, Wawa–Abitibi terrane, Superior Province, northwestern Ontario; Ontario Geological Survey, Miscellaneous Release—Data 382.

Heaman, L.M. 1997. Global mafic magmatism at 2.45 Ga: Remnants of an ancient large igneous province?; Geology, v.25, p.299-302.

Heaman, L.M. and Easton, R.M. 2006. Preliminary U-Pb geochronology results from the Lake Nipigon Region Geoscience Initiative; Ontario Geological Survey, Miscellaneous Release—Data 191.

Heaman, L.M. and Machado, H. 1992. Timing and origin of Midcontinent Rift alkaline magmatism, North America: Evidence from the Coldwell complex; Contributions to Mineralogy and Petrology, v.110, p.289-303.

Hollings, P., Fralick, P. and Cousens, B. 2007. Early history of the Midcontinent Rift inferred from geochemistry and sedimentology of the Mesoproterozoic Osler Group, northwestern Ontario; Canadian Journal of Earth Sciences, v.44, p.389-412.

Irvine, T.N. and Baragar, W.R.A. 1971. A guide to the chemical classification of the common volcanic rocks; Canadian Journal of Earth Sciences, v.8, p.523-548.

Kamo, S.L. 2016. Report on U-Pb ID-TIMS geochronology for the Ontario Geological Survey: Bedrock mapping projects, Ontario; internal report for the Ontario Geological Survey, Jack Satterly Geochronology Laboratory, University of Toronto, Toronto, Ontario, 63p.

——— 2019a. Part A: Report on U-Pb ID-TIMS geochronology for the Ontario Geological Survey: Bedrock mapping projects, Ontario, Year 4: 2018–2019; internal report for the Ontario Geological Survey, Jack Satterly Geochronology Laboratory, University of Toronto, Toronto, Ontario, 25p.

——— 2019b. U-Pb CA-D-TIMS zircon age for tonalite sample 18SJM-087, Priske Township, Ontario; internal report for the Ontario Geological Survey, Jack Satterly Geochronology Laboratory, University of Toronto, Toronto, Ontario, 4p.

Kamo, S.L. and Hamilton, M.A. 2017. Part A: Report on U-Pb ID-TIMS geochronology for the Ontario Geological Survey: Bedrock mapping projects, Ontario, Year 2: 2016–2017; internal report prepared for the Ontario Geological Survey, Jack Satterly Geochronology Laboratory, University of Toronto, Toronto, Ontario, 72p. with updated data for samples 15JW005, 15JW132, and 15JW150 provided in June 2021.

——— 2018. Part A: Report on U-Pb ID-TIMS geochronology for the Ontario Geological Survey: Bedrock mapping projects, Ontario, Year 3: 2017–2018; internal report for the Ontario Geological Survey; Jack Satterly Geochronology Laboratory, University of Toronto, Toronto, Ontario, 44p.

Le Maitre, R.W., ed. 1989. A classification of igneous rocks and glossary of terms; Blackwell Scientific Publications, Oxford, United Kingdom, 193p.

Lesher, C.M., Goodwin, A.M., Campbell, I.H. and Gorton, M.P. 1986. Trace-element geochemistry of ore-associated and barren, felsic metavolcanic rocks in the Superior Province, Canada; Canadian Journal of Earth Sciences, v.23, p.222-237.

Liikane, D.A., Bleeker, W., Hamilton, M., Kamo, S., Smith, J., Hollings, P., Cundari, R. and Easton, M. 2018. Controls on the localization and timing of mineralized intrusions within the ca. 1.1 Ga Midcontinent Rift system; 64th Institute on Lake Superior Geology, Proceedings, v.64, pt.1, p.65-66.

Lodge, R.W.D., Gibson, H.L., Stott, G.M., Franklin, J.M. and Hamilton, M.A. 2014. Geodynamic reconstruction of the Winston Lake greenstone belt and VMS deposits: New trace element geochemistry and U-Pb geochronology; Economic Geology, v.109, p.1291-1313.

Magnus, S.J. 2017a. Precambrian geology of Tuuri and Walsh townships, northwestern Ontario; Ontario Geological Survey, Preliminary Map P.3812, scale 1:20 000.

——— 2017b. Geology and mineral potential of Syine Township, western Schreiber–Hemlo greenstone belt; *in* Summary of Field Work and Other Activities, 2017, Ontario Geological Survey, Open File Report 6333, p.11-1 to 11-8.

——— 2018. Geological, geochemical, geophysical and petrographic data from Tuuri and Walsh townships, Schreiber–Hemlo greenstone belt, Wawa–Abitibi terrane, Superior Province; Ontario Geological Survey, Miscellaneous Release—Data 361.

——— 2019a. Precambrian geology, Syine Township; Ontario Geological Survey, Preliminary Map P.3826, scale 1:20 000.

——— 2019b. Geological, geochemical and petrographic data from Syine Township, western Schreiber–Hemlo greenstone belt, Wawa–Abitibi terrane, Superior Province, northwestern Ontario; Ontario Geological Survey, Miscellaneous Release—Data 375.

——— 2019c. Geology of the western Schreiber–Hemlo greenstone belt: A geological guidebook; Ontario Geological Survey, Open File Report 6357, 41p.

——— 2021a. Precambrian geology of Priske Township, northwestern Ontario; Ontario Geological Survey, Preliminary Map P.3845, scale 1:20 000.

——— 2021b. Geological, geochemical and petrographic data from Priske Township and Nd, Sm and Sr isotopic data from Priske, Strey, Syine, Tuuri and Walsh townships, Western Schreiber–Hemlo greenstone belt, Wawa–Abitibi terrane, Superior Province, northwestern Ontario; Ontario Geological Survey, Miscellaneous Release—Data 381.

——— 2021c. Chemostratigraphy of the western Schreiber–Hemlo greenstone belt: Results and regional implications; 67th Institute on Lake Superior Geology, Proceedings, v.67, pt.1, p.44-45.

——— 2021d. Proterozoic geology of the Schreiber–Terrace Bay area; 67th Institute on Lake Superior Geology, Proceedings, v.67, pt.1, p.46-47.

Magnus, S.J. and Arnold, K.A. 2016. Geology and mineral potential of the western Schreiber–Hemlo greenstone belt; *in* Summary of Field Work and Other Activities, 2016, Ontario Geological Survey, Open File Report 6323, p.11-1 to 11-7.

Magnus, S.J. and Hastie, E.C.G. 2018. Geology and mineral potential of Priske and Strey townships, western Schreiber–Hemlo greenstone belt; *in* Summary of Field Work and Other Activities, 2018, Ontario Geological Survey, Open File Report 6350, p.10-1 to 10-10.

Magnus, S.J. and Walker, J. 2015. Geology and mineral potential of Walsh, Tuuri and Syine townships, Schreiber–Hemlo greenstone belt; *in* Summary of Field Work and Other Activities, 2015, Ontario Geological Survey, Open File Report 6313, p.14-1 to 14-12.

Meghji, I. 2016. The character and distribution of Cu-PGE mineralization at the Geordie Lake Deposit within the Coldwell Complex, Ontario; unpublished MSc thesis, University of Western, Ontario, London, Canada, 336p.

Miller, J.D. and Nicholson, S.W. 2013. Geology and mineral deposits of the 1.1 Ga Midcontinent Rift in the Lake Superior region—An overview; *in* Field Guide to the Cu-Ni-PGE Deposits of the Lake Superior Region, Precambrian Research Center Guidebook 13-1, University of Minnesota Press, p.1-50.

Muir, T.L. 2003. Structural evolution of the Hemlo greenstone belt in the vicinity of the world-class Hemlo gold deposit; Canadian Journal of Earth Sciences, v.40, p.395-430.

Ojakangas, R.W., Morey, G.B. and Southwick, D.L. 2001. Paleoproterozoic basin development and sedimentation in the Lake Superior region, North America; Sedimentary Geology, v.141-142, p.319-341.

Ontario Geological Survey 2003. Ontario airborne geophysical surveys, magnetic and electromagnetic data, Schreiber area; Ontario Geological Survey, Geophysical Data Set 1104—Revised.

——— 2011. 1:250 000 scale bedrock geology of Ontario; Ontario Geological Survey, Miscellaneous Release—Data 126 – Revision 1.

——— 2019. GeochrON. Geochronology Inventory of Ontario (compilation); Ontario Geological Survey, OGSEarth online database, July 2019 beta version, accessed October 16, 2019.

Plank, T. 2005. Constraints from thorium/lanthanum on sediment recycling at subduction zones and the evolution of the continents; Journal of Petrology, v.46, p.921-944.

Rogala, B., Fralick, P.W. and Metsaranta, R. 2005. Stratigraphy and sedimentology of the Mesoproterozoic Sibley Group and related igneous intrusions, northwestern Ontario: Lake Nipigon Region Geoscience Initiative; Ontario Geological Survey, Open File Report 6174, 128p.

Ross, P-S. and Bédard, J.H. 2009. Magmatic affinity of modern and ancient subalkaline volcanic rocks determined from trace element discriminant diagrams; Canadian Journal of Earth Sciences, v.46, p.823-839.

Rukhlov, A.S. and Bell, L. 2010. Geochronology of carbonatites from the Canadian and Baltic shields, and the Canadian Cordillera: Clues to mantle evolution; Mineralogy and Petrology, v.98, p.11-54.

Scott, D.J. and St-Onge, M.R. 1995. Constraints on Pb closure temperature in titanite based on rocks from the Ungava Orogen, Canada: Implications for U-Pb geochronology and P-T-t path determinations; Geology, v.23, p.1123-1126.

Stott, G.M., Corkery, M.T., Percival, J.A., Simard, M. and Goutier, J. 2010. Revised terrane subdivision of the Superior Province; *in* Summary of Field Work and Other Activities, 2010, Ontario Geological Survey, Open File Report 6260, p.20-1 to 20-10.

Sun, S. -s. and McDonough, W.F. 1995. The composition of the Earth; Chemical Geology, v.120, p.223-253.

Sutcliffe, C.N. and Davis, D.W. 2019. U-Pb geochronology by LA-ICP-MS in samples from northern Ontario; internal report prepared for the Ontario Geological Survey, Jack Satterly Geochronology Laboratory, University of Toronto, Toronto, Ontario, 146p.

Tóth, Z. 2018. The geology of the Beardmore–Geraldton belt, Ontario, Canada: Geochronology, tectonic evolution and gold mineralization; unpublished PhD thesis, Laurentian University, Sudbury, Ontario, 276p.

Tóth, Z., Lafrance, B., Dube, B., McNicoll, V.J., Mercier-Langevin, P. and Creaser, R.A. 2015. Banded iron formation-hosted gold mineralization in the Geraldton area, northwestern Ontario: Structural setting, mineralogical characteristics, and geochronology; *in* Targeted Geoscience Initiative 4: Contributions to the Understanding of Precambrian Lode Gold Deposits and Implications for Exploration; Geological Survey of Canada, Open File 7852, p.85-97.

Wacey, D., McLoughlin, N., Kilburn, M.R., Saunders, M., Cliff, J.B., Kong, C., Barley, M.E. and Brasier, M.D. 2013. Nanoscale analysis of pyritized microfossils reveals differential heterotrophic consumption in the ~1.9-Ga Gunflint chert; Proceedings of the National Academy of Sciences of the United States of America, v.110, no.20, p.8020-8024.

Whitmeyer, S.J. and Karlstrom, K.E. 2007. Tectonic model for the Proterozoic growth of North America; Geosphere, v.3, no.4, p.220-259.

Williams, H.R. 1989. Geological studies of the Wabigoon, Quetico and Abitibi–Wawa subprovinces, Superior Province of Ontario, with emphasis on the structural development of the Beardmore–Geraldton belt; Ontario Geological Survey, Open File Report 5724, 189p.

Workman, R.H. and Hart, S.R. 2005. Major and trace element composition of the depleted MORB mantle (DMM); Earth and Planetary Science Letters, v.231, p.53-72.

Wu, F-Y, Mitchell, R.H., Li, Q-L, Zhang, C. and Yang, Y-H. 2017. Emplacement age and isotopic composition of the Prairie Lake carbonatite complex, northwestern Ontario, Canada; Geological Magazine, v.154, no.2, p.217-236.

Zaleski, E., van Breemen, O. and Peterson, V.L. 1999. Geological evolution of the Manitouwadge greenstone belt and Wawa–Quetico subprovince boundary, Superior Province, Ontario, constrained by U-Pb zircon dates of supracrustal and plutonic rocks; Canadian Journal of Earth Sciences, v.36, p.945-966.

Metric Conversion Table

Conversion from SI to Imperial			Conversion from Imperial to SI		
SI Unit	*Multiplied by*	*Gives*	*Imperial Unit*	*Multiplied by*	*Gives*
		LENGTH			
1 mm	0.039 37	inches	1 inch	**25.4**	mm
1 cm	0.393 70	inches	1 inch	**2.54**	cm
1 m	3.280 84	feet	1 foot	**0.304 8**	m
1 m	0.049 709	chains	1 chain	20.116 8	m
1 km	0.621 371	miles (statute)	1 mile (statute)	**1.609 344**	km
		AREA			
1 cm^2	0.155 0	square inches	1 square inch	**6.451 6**	cm^2
1 m^2	10.763 9	square feet	1 square foot	**0.092 903 04**	m^2
1 km^2	0.386 10	square miles	1 square mile	2.589 988	km^2
1 ha	2.471 054	acres	1 acre	0.404 685 6	ha
		VOLUME			
1 cm^3	0.061 023	cubic inches	1 cubic inch	**16.387 064**	cm^3
1 m^3	35.314 7	cubic feet	1 cubic foot	0.028 316 85	m^3
1 m^3	1.307 951	cubic yards	1 cubic yard	0.764 554 86	m^3
		CAPACITY			
1 L	1.759 755	pints	1 pint	0.568 261	L
1 L	0.879 877	quarts	1 quart	1.136 522	L
1 L	0.219 969	gallons	1 gallon	**4.546 090**	L
		MASS			
1 g	0.035 273 962	ounces (avdp)	1 ounce (avdp)	28.349 523	g
1 g	0.032 150 747	ounces (troy)	1 ounce (troy)	**31.103 476 8**	g
1 kg	2.204 622 6	pounds (avdp)	1 pound (avdp)	**0.453 592 37**	kg
1 kg	0.001 102 3	tons (short)	1 ton(short)	**907.184 74**	kg
1 t	1.102 311 3	tons (short)	1 ton (short)	**0.907 184 74**	t
1 kg	0.000 984 21	tons (long)	1 ton (long)	**1016.046 908 8**	kg
1 t	0.984 206 5	tons (long)	1 ton (long)	**1.016 046 9**	t
		CONCENTRATION			
1 g/t	0.029 166 6	ounce (troy) / ton (short)	1 ounce (troy) / ton (short)	34.285 714 2	g/t
1 g/t	0.583 333 33	pennyweights / ton (short)	1 pennyweight / ton (short)	1.714 285 7	g/t

OTHER USEFUL CONVERSION FACTORS

	Multiplied by	
1 ounce (troy) per ton (short)	31.103 477	grams per ton (short)
1 gram per ton (short)	0.032 151	ounces (troy) per ton (short)
1 ounce (troy) per ton (short)	20.0	pennyweights per ton (short)
1 pennyweight per ton (short)	0.05	ounces (troy) per ton (short)

*Note: Conversion factors in **bold** type are exact. The conversion factors have been taken from or have been derived from factors given in the* Metric Practice Guide for the Canadian Mining and Metallurgical Industries*, published by the Mining Association of Canada in co-operation with the Coal Association of Canada.*

ISSN 0826-9580 (print)
ISBN 978-1-4868-5603-9 (print)

ISSN 1916-6117 (online)
ISBN 978-1-4868-5604-6 (PDF)